ATTENUATION CONCEPT FOR EVALUATING RELEASE OF RADIOIODINE FOLLOWING A LOSS-OF-COOLANT ACCIDENT

D. H. Walker

Idaho Nuclear Corporation
National Reactor Testing Station
Idaho Falls, Idaho

ABSTRACT

In evaluating the suitability of pressurized water reactor sites in the United States, the release of radioactivity in the event of a loss-of-coolant accident is one of the major considerations. Doses from released radioactivity at the site boundary must be shown to be less than the guidelines set forth in Title 10, Part 100 of the Code of Federal Regulations. For the loss-of-coolant accident, the criteria in the guidelines regarding radioiodine isotopes are most restrictive at the site boundary. In this paper, the effects of various processes, including those of reactor safety system operation, on the amount of radioiodine escaping from the reactor containment vessel are discussed.

The fission product iodine activity generated in the nuclear core during reactor operation represents the source of activity available for release in the event of a loss-of-coolant accident. However, various processes, such as retention of radioactivity within the nuclear fuel, deposition of radioactivity on core and reactor system surfaces, absorption by core cooling water, and deposition on containment surfaces serve to reduce the amount of radioiodine which reaches the environment. Active reactor safety systems, such as reactive containment sprays and the containment filter system, and the passive containment pressure barrier also serve to reduce the amount of radioiodine leaking to the environment.

Estimates of the magnitude of the radioiodine attenuation and the uncertainties associated with the estimates for each of the sequential events in the transport of radioactivity from the fuel through the containment to the environment can be conveniently represented on an iodine attenuation diagram. The distances to the site boundary needed to meet dose guidelines for specified weather conditions can also be represented on the diagram to assist in evaluating the adequacy of a reactor site.

Iodine attenuation diagrams are presented for a typical large pressurized-water reactor. Iodine attenuation by various processes or safety systems, during each of the events in the radioiodine transport sequence, is indicated for the maximum credible loss-of-coolant accident condition (as defined in Title 10, Section 100 of the Code of Federal Regulations), and for expected loss-of-coolant accident conditions.

Programs now planned or in progress in the United States for studying radioiodine release and behavior in a loss-of-coolant accident are summarized and briefly discussed. These programs include the development of analytical methods for describing the release and behavior of radioiodine, experiments to study radioiodine behavior in the individual events of the iodine transport sequence, and large-scale experiments to study the overall transport sequence in conjunction with loss-of-coolant accident tests to be conducted in the Loss-of-Fluid-Test (LOFT) Facility. The potential of these programs for providing an additional margin of assurance relative to radioiodine release in a loss-of-coolant accident is discussed. The additional iodine attenuation that might be realized from these programs is indicated on an iodine attenuation diagram.

Introduction

In evaluating the suitability of pressurized water reactor sites in the United States, the release of radioactivity in the event of a loss-of-coolant accident is one of the major considerations. For a site to be acceptable, doses from released radioactivity at the site boundary must be shown to meet the siting criteria set forth in Title 10, Part 100 of the Code of Federal regulations[1].

Operating pressurized water reactors have three basic barriers to minimize the release of fission products from the reactor plant to the environment. These barriers are the fuel element cladding, the primary system of the reactor plant, and the containment vessel that surrounds the reactor plant. In the event of a loss-of-coolant accident, the primary system is ruptured and at least limited failure of the fuel element cladding is likely. The containment vessel is then the remaining basic barrier for limiting release of fission products to the environment.

For a loss-of-coolant accident, the most restrictive of the criteria in the guidelines are those regarding the dose to the thyroid as a result of inhalation of radioiodine. The I-131 release from the containment that will produce a thyroid dose of 300 rem after two hours of inhalation is plotted as a function of distance from the containment vessel on Figure 1. The plot is for Pasquill type F weather conditions. Also included on the plot is the equivalent whole body dose for a two-hour exposure to the cloud of released radioactive material. The whole body dose was estimated by assuming:

(1) The radioactive source in the containment vessel atmosphere contains 100% of the core noble gas inventory and 25% of the core iodine inventory as specified by TID-14844[2].

(2) The noble gases and iodine activities leak from the containment vessel and appear in the environment in the same ratio as they are present in the containment atmosphere. Thus, the indicated whole body dose is based on a fission product source whose activities are present in a specific ratio.

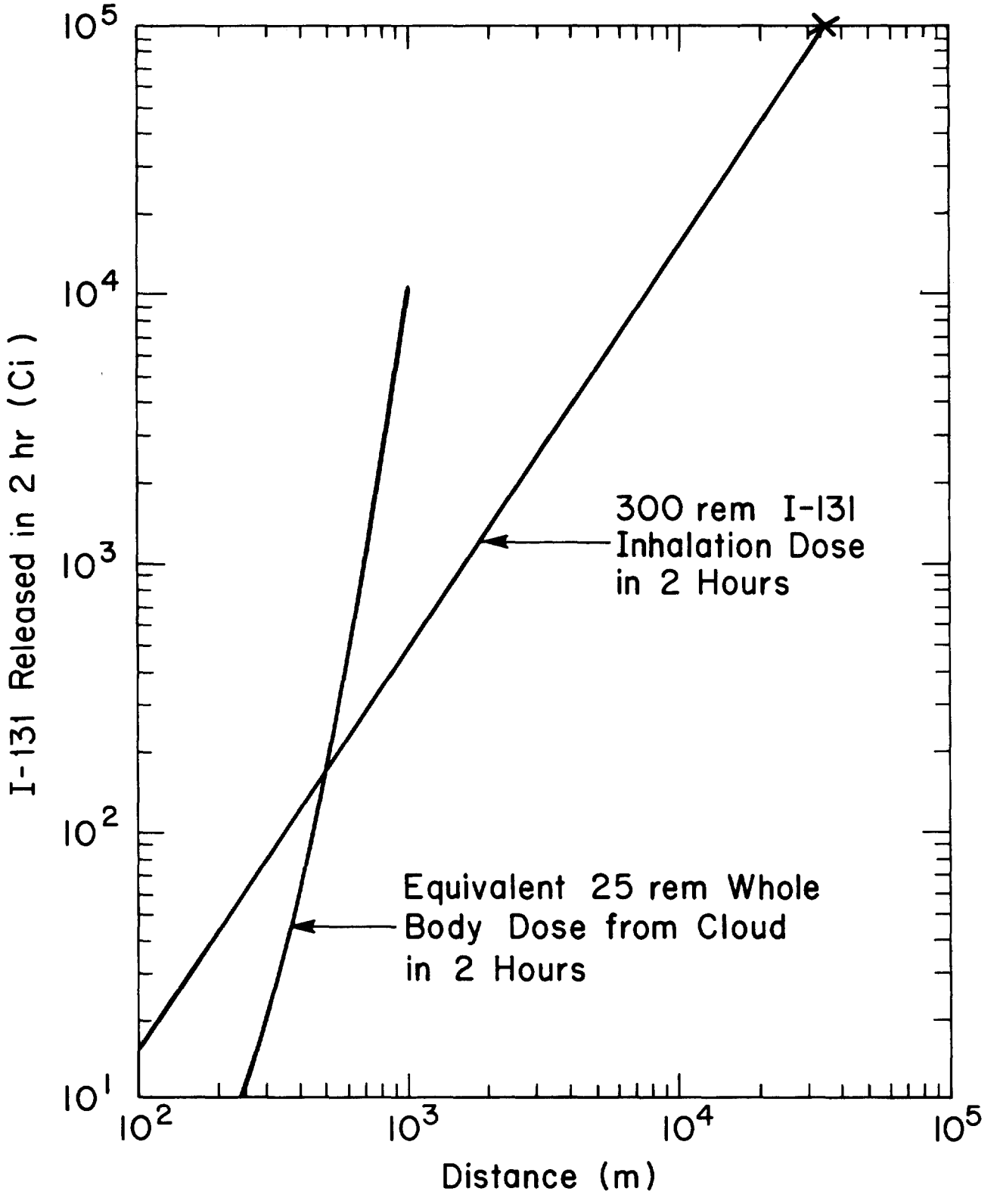

INC-A-15147

FIGURE 1 EXCLUSION RADIUS AS A FUNCTION OF I-131 RELEASE FOR A LOSS-OF-COOLANT ACCIDENT

Figure 1 shows that for exclusion distances greater than about 500 meters, the thyroid inhalation dose limit is reached before the whole body dose limit. The I-131 release from the containment that would produce the 300-rem thyroid dose at 500 meters is only about 200 curies. For large power reactors, current guidelines for estimating iodine release in the event of a maximum hypothetical loss-of-coolant accident[2] indicate the potential for I-131 release is substantially larger than 200 curies. Thus, guidelines regarding the dose to the thyroid from inhalation of I-131 are generally more limiting with respect to the consequences of the accident than are the whole body dose guidelines.

Figure 2 is plot analogous to Figure 1 for the low population zone radius. The iodine-131 release from the containment that will produce a thyroid dose of 300 rem from inhalation of radioiodine during the total passage of the released radioactive cloud is plotted as a function of distance. The plot is for Pasquill type F weather. Also included on Figure 2 is a plot of the equivalent whole body dose for exposure during the total passage of the cloud of released radioactive material.

Iodine Attenuation Diagram

The fission product iodine activity generated in the nuclear core during reactor operation represents the source of activity available for release in the event of a loss-of-coolant accident. However, various processes, such as retention of radioactivity within the nuclear fuel, deposition of radioactivity on core and reactor system surfaces, absorption by core cooling water, and deposition on containment surfaces serve to reduce the amount of radioiodine that reaches the environment. Active reactor safety systems, such as reactive containment sprays and the containment filter system, and the passive containment pressure barrier also serve to reduce the amount of radioiodine leaking to the environment.

Estimates of the magnitude of the radioiodine attenuation for each of the sequential events in the transport of radioactivity from the fuel through the containment to the environment and the uncertainties associated with the estimates can be represented on an iodine attenuation diagram. The distances to the site boundary needed to meet the dose guidelines of Reference 1 can also be represented on the diagram for specified weather conditions to assist in evaluating the adequacy of a reactor site.

Figure 3 is an I-131 attenuation diagram for a 1000 MW(e) water-moderated reactor plant. Represented across the top of the diagram are the various steps in the migration of iodine from the core to the environment following a loss-of-coolant accident. As indicated, part of the core iodine inventory migrates from the fuel to the plenum space of the fuel pin during reactor operation. Some fraction is released upon cladding rupture and is transported to the containment vessel. Application of sprays, containment filter systems, or other

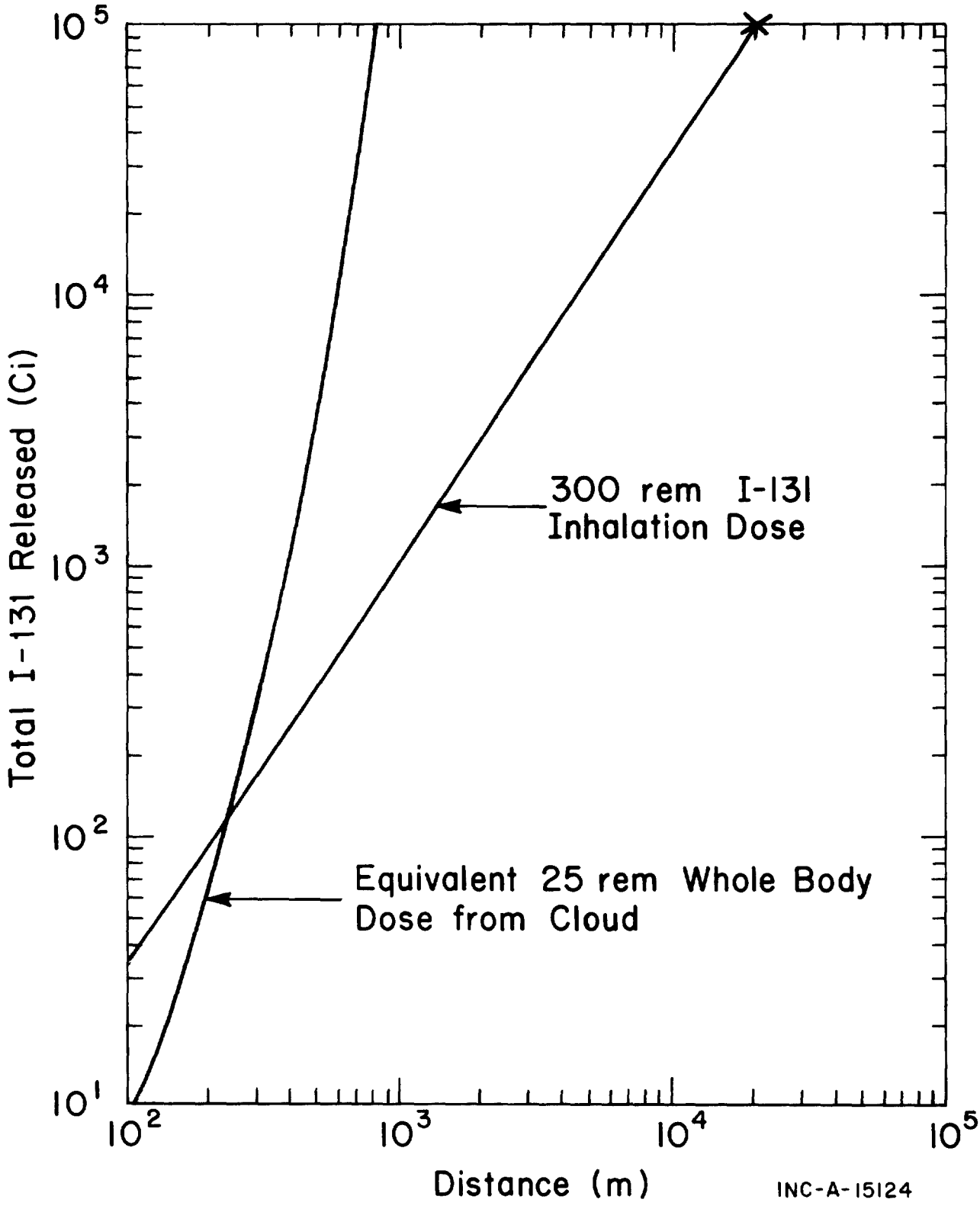

FIGURE 2 LOW POPULATION RADIUS AS A FUNCTION OF I-131 RELEASE FOR LOSS-OF-COOLANT ACCIDENT

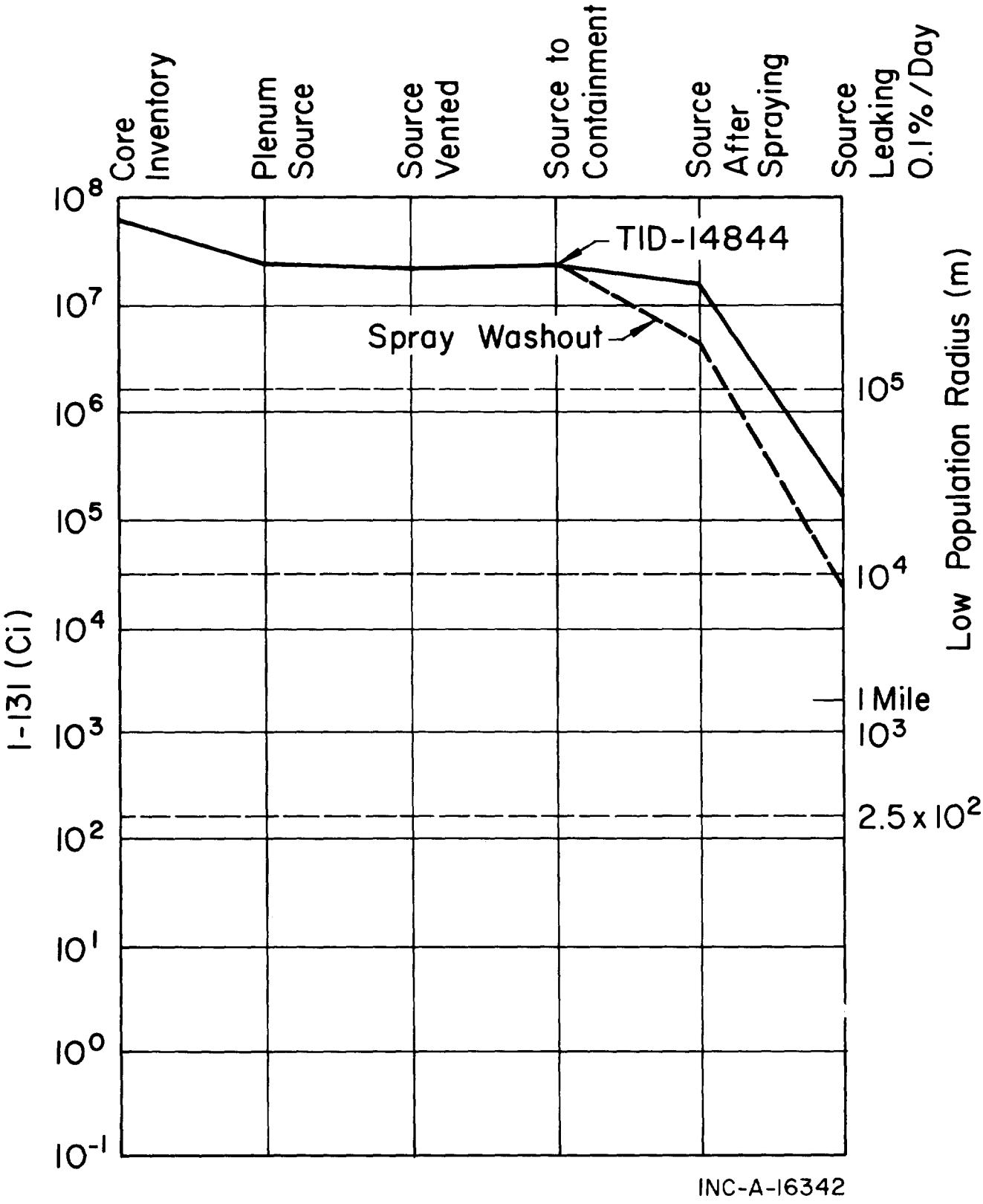

FIGURE 3 I-131 ATTENUATION DIAGRAM FOR MAXIMUM HYPOTHETICAL ACCIDENT FOR A 1000 MW(e) REACTOR

iodine cleanup systems further reduces the iodine source in the containment vessel that is available for leakage across the containment shell to the environment. Indicated on the left side of the diagram is the magnitude of the iodine source in curies. The corresponding low population zone radius is indicated on the right hand side. The correspondence between curies of iodine and low population zone radius is derived from Figure 2.

Also indicated on Figure 3 is a line showing iodine attenuation representative of current practice in evaluating iodine release following a maximum hypothetical loss-of-coolant accident (MHA). The guidelines for evaluating iodine release following an MHA appear in TID-14844. The guidelines indicate that one half of the core iodine source should be considered as available for release in the event of the MHA. Of the iodine available for release, one half should then be considered to remain in the containment atmosphere as a long-term source. Current practice in evaluating the consequences of an MHA is to assume that iodine attenuation provided by containment sprays is no greater than a factor of ten. The spray attenuation factor has been indicated on Figure 2 by a dotted line. When the guidelines of TID-14844 are applied for the MHA condition, the containment barrier provides about an additional factor of 100 iodine attenuation. Thus, 10^4 to 10^5 curies of iodine could reach the environment in the event of an MHA. A low population zone radius of one to ten miles is required to meet the dose guidelines of Reference 1.

Figure 4 is a diagram on which an estimate of the attenuation potentially attainable from a better understanding of iodine migration following a loss-of-coolant accident has been indicated by the lower attenuation curve. The vertical bars associated with the lower attenuation curve are an indication of the uncertainty associated with the estimate of the attenuation attainable from that step in the iodine transport process. For example, the diagram indicates one decade as the potentially identifiable attenuation for the process of the iodine migration from the fuel to the fuel pin plenum during reactor operation. The diagram also indicates a one and one half decade uncertainty associated with this estimate. Similarly for application of containment sprays, the diagram indicates two and one half decades as the potentially identifiable attenuation. A possible two-decade uncertainty is indicated on the diagram. Current practice is to apply one decade attenuation or less in evaluating this step of the iodine transport process.

The lower line on Figure 3 indicates the possibility that iodine release from the containment vessel of a pressurized water reactor following a loss-of-coolant accident might actually be less than ten curies. However, uncertainties in the current state of knowledge concerning iodine behavior make application of conservative attenuation values necessary for each step in the iodine attenuation process. Thus, iodine release values of 10^4 to 10^5 are used in evaluating the adequacy of a reactor site relative to the consequences of a loss-of-coolant accident. The purpose of analytical and experimental studies of the

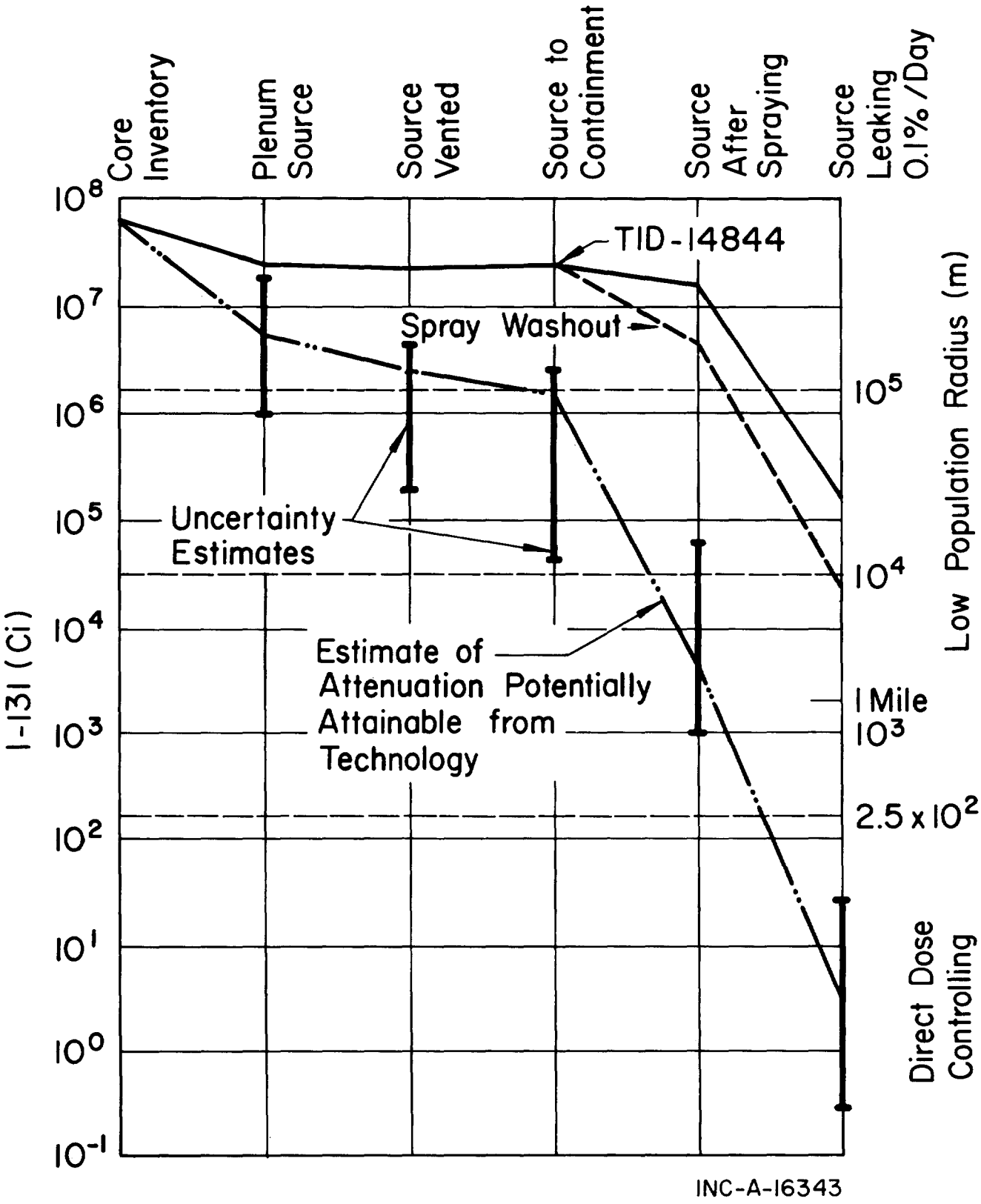

FIGURE 4 I-131 ATTENUATION DIAGRAM FOR 1000 MW(e) REACTOR

release and subsequent behavior of radioiodine in a loss-of-coolant accident is to reduce the uncertainty associated with iodine attenuation behavior during its transport from the core to the environment following a loss-of-coolant accident.

Figures 3 and 4 are attenuation diagrams for a large pressurized water reactor. Similar diagrams could also be drawn readily for boiling water reactors.

Iodine Behavior Programs

A number of experimental and analytical programs are currently planned or in progress in the United States for studying radioiodine release and behavior in a loss-of-coolant accident. The programs can be related to the steps in the iodine migration sequence represented across the top of the iodine attenuation diagram, Figure 3.

1. Plenum Source

During operation of the reactor, some fraction of the more volatile fission products generated in the fuel such as noble gases and iodine, migrate from the fuel rod plenum. Fission products in the fuel rod plenum are available for release from the fuel pin upon rupture of the cladding. If the emergency core cooling systems of the current large pressure water reactors function is designed, the core thermal transient that follows a loss-of-coolant accident will be terminated before the core overheats sufficiently to drive off significant additional fission products. However, cladding rupture of at least some fuel pins is likely. Thus, fission products present in the fuel pin plenum prior to the loss-of-coolant accident represent the probable fission product source available for release.

In evaluating the consequences of a maximum hypothetical accident, one half of the core radioiodine inventory is assumed present in the fuel rod plenum and available for release following a loss-of-coolant accident[2]. Additional information regarding fission product migration during reactor operation may show that an attenuation factor of ten is associated with this step in the iodine migration chain for current reactors. However, future reactors of higher fuel power density are likely to exhibit lower attenuation factors for this step in the migration chain.

Unresolved issues relative to the migration of fission products from the fuel to the fuel rod plenum during reactor operation are indicated in Table I. The status of experimental data and the describing analysis as well as needs for experimental and analytical programs are also indicated.

TABLE I

FISSION PRODUCT RELEASE --
PROGRAM AND REQUIREMENTS SUMMARY

ISSUE	STATUS	NEEDS		PROGRAMS	
		Experimental	Model	Experimental	Model
Gas Migration to Plenum	Much Experimental Data, Need Better Model	Limited Program	Needed	Planned INC	In Progress INC
Iodine Migration to Plenum	Little Data No Model	Needed	Needed	None	Planned INC
Release from Overheated Fuels	Much Data Models Exist	None	None	None	None

Current and planned programs related to the migration of fission products from the fuel to the fuel rod plenum during reactor operation are the following:

(a) An Idaho Nuclear Corporation program to develop an analytical model for describing the migration of fission product noble gases and iodine in UO_2 in the presence of a thermal gradient. The model will be based on a chemical free energy approach[3],

(b) A planned program at Idaho Nuclear Corporation for measuring the migration of noble gases across ceramic membranes in the presence of an applied thermal gradient[4].

2. Venting and Transport Through the Reactor System

Following rupture of the fuel pin cladding some fraction of the radioiodine in the fuel pin plenum will be vented from the plenum and transported through the reactor system to the containment vessel. Processes that will function to reduce the amount of radioiodine reaching the containment vessel include:

(a) Retention within the fuel pin due to adsorption on cladding surfaces and retention along the tortuous migration paths to the point of cladding rupture,

(b) Adsorption of iodine on core cladding surfaces, surfaces of core structural materials, and surfaces of the reactor system,

(c) Retention of iodine by reactor coolant and injected emergency core cooling water.

Little information is available on the fraction of radioiodine that will be vented following a loss-of-coolant accident or the fraction retained by system surfaces and cooling water. In the absence of information, the assumption usually made in evaluating an MHA is that all of the radioiodine available in the fuel plenum is vented upon cladding rupture and all of the vented radioiodine reaches the containment. Additional information concerning venting following cladding rupture and the retention of fission products by system surfaces and cooling water may well show that attenuation factors in the range of 10 to 1000 are associated with these processes in the fission product migration chain, as indicated on Figure 4.

Unresolved issues relative to radioiodine venting and the transport of radioiodine through the reactor system are indicated in Table II. The status of experimental data and the describing analysis as well as experimental data and analytical development needs are also indicated on the figure.

Current and planned programs related to the venting of radioiodine and the transport of radioiodine through the reactor system are the following:

(a) An experimental program to study the venting of radioiodine upon fuel pin cladding rupture, and to study the transport of fission products through a simulated reactor system is planned for the Containment Research Installation Facility at Oak Ridge National Laboratory[4]. The capability to introduce emergency core cooling water by either bottom flooding or by sprays mounted above a simulated fuel bundle is included in the experimental facility.

TABLE II

SOURCE ATTENUATION BY VENTING AND TRANSPORT TO CONTAINMENT -- PROGRAM AND REQUIREMENTS SUMMARY

ISSUE	STATUS	NEEDS		PROGRAMS	
		Experimental	Model	Experimental	Model
Iodine Venting	Limited Data TREAT[5]	Needed	Needed	Planned CRI-ORNL LOFT	Planned INC
Noble Gas Venting	Limited Data TREAT[5]	Limited	Limited	Planned TREAT LOFT	None
Iodine Retention by ECC and System Surfaces	No Data	Needed	Needed	Planned CRI-ORNL LOFT	Planned INC
UO_2 Venting and Transport	Qualitative Data	Needed	None	Planned CRI-TREAT LOFT	None

(b) Limited information concerning the venting of noble gases upon fuel pin rupture will be obtained as part of the TREAT fuel rod failure tests being conducted by Oak Ridge National Laboratory[5].

(c) Data concerning radioiodine retention by ruptured fuel pins and the retention of radioiodine by reactor system surfaces and core cooling water will be obtained as part of the experimental program to be considered in the Loss-of-Fluid-Test (LOFT) Facility[6].

(d) A program to develop an analytical method for predicting the retention fractions associated with radioiodine venting and transport retention is planned in conjunction with the Containment Research Installation Experimental Program. The analytical development program will be conducted by Idaho Nuclear Corporation[3].

3. Attenuation by Containment Processes

Radioiodine in the containment atmosphere represents the iodine source available for leakage from the containment to the environment. By reducing the quantity of radioiodine in the containment atmosphere, the quantity of iodine leaking to the environment can also be reduced. Thus, systems have been incorporated into the containment that serve to remove iodine from the containment atmosphere. These systems include spray scrubbing systems that employ solutions with chemical additives, and air circulating systems that contain specific adsorbers for iodine. In addition, natural processes also remove radioiodine from the containment atmosphere. However, removal rates for natural processes are substantially less than are the iodine removal rates associated with the active, engineered system.

In current reactor licensing considerations, iodine attenuation factors attributable to spray systems and recirculating adsorber system are limited to no more than a factor of 10. The limited attenuation is a result of experimental observations that show that some fraction of the radioiodine in the containment atmosphere is present as persistent species that are not readily scrubbed from the containment atmosphere by spray systems, nor are they readily adsorbed on standard materials for adsorbing molecular iodine. The persistent species appear to be principally methyl iodide and hypoiodous acid[7,8]. Additional information concerning the relationships between molecular iodine and the persistent forms of radioiodine, may show that iodine attenuation factors of 100 to 1000 are attainable when containment systems for iodine removal are applied.

Issues relative to the behavior of radioiodine in the containment are indicated in Table III. The status of experimental information and describing analysis relative to each of the issues are indicated, as are needs for additional analytical and experimental programs.

Current and planned programs related to the behavior of radioiodine in the containment atmosphere and the effect of engineered safety systems on this behavior are the following:

(a) A combined experimental and analytical program to determine the effect of the iodine mass level concentration, containment atmospheric contaminants, and the composition of solutions in the containment on the fraction of radioiodine present as persistent species. Washout of hypoiodous acid by sprays probably will be included as part of this program[4,7].

(b) A program to develop and study the capabilities of metal zeolites to retain both molecular iodine and persistent iodine species[9]. This program is being conducted by Idaho Nuclear Corporation.

(c) A recently completed program in the Containment Systems Experiments (CSE) Facility at Battelle Northwest Laboratory in which the removal of iodine and particulate fission products was measured[10].

TABLE III

CONTAINMENT PROCESSES --
PROGRAM AND REQUIREMENTS SUMMARY

ISSUE	STATUS	NEEDS		PROGRAMS	
		Experimental	Model	Experimental	Model
Fraction as Persistent Gas-Phase Iodine	Some Data Available	Needed	Needed	In Progress INC	In Progress INC
Fraction as Persistent Particulate Iodine	Data Limited	Needed	Probable	Some Data From CRI, LOFT	None
Spray Washout Reaction Iodine	Data and Models Available	Available	Available	CSE NSPP	BNWL ORNL
Spray Washout Organic Iodine	Data and Models Available	Available	Available	CSE NSPP	BNWL ORNL
Spray Washout HOI	No Data or Models	Probable	Probable	None	Planned INC
Spray Washout Particles	Models and Some Data	Available[(a)]	Available[(a)]	CSE NSPP	BNWL ORNL
Particle Size and Number Densities	No Data for ECC Condition	Needed	Probable	Currently None (CRI-LOFT)	None
Filter Retention Persistent Iodine	Current Experiments	Needed	None	CSE INC New Material	None
Filter Retention - Particles	Current Experiments	Needed	None	Limited CSE	None
Natural Deposition - Main Chamber	Programs Completed	Available	Available	CRI, CDE, CSE	INC BNWL
Natural Deposition - Compartments	Some Data	Available	Yes	CSE, CVTR	Planned INC

[(a)] Data on Particle Size Distribution Needed

SUMMARY AND CONCLUSIONS

In the unlikely event a pressurized water nuclear reactor undergoes a loss-of-coolant accident, some fraction of the core fission product inventory will very probably be released, transported to the containment, and some small fraction of the fission products reaching the containment will leak to the environment. The dose to the thyroid resulting from inhalation of radioiodine represents the greatest potential radiological hazard from the released fission product radioactivity.

One method of representing the fraction of the core radioiodine inventory that might reach the environment is an iodine attenuation diagram. The fraction of the iodine removed in each of the processes in the transport of iodine from the core, through the reactor system to the containment, and through the containment to the environment can be represented on the diagram. Various assumptions regarding radioiodine removal in a particular process of the transport chain can be evaluated quickly through use of the diagram.

The attenuation diagrams presented in the paper show that application of current guidelines for evaluating radioiodine behavior following a maximum hypothetical loss-of-coolant accident[1,2] produces estimates for release of I-131 to the environment of 10^4 to 10^5 curies. The diagrams also show that additional effort to produce a better understanding of iodine behavior may lead to estimates as low as 10 curies for I-131 release to the environment following a loss-of-coolant accident. These attenuation diagrams indicate that a substantial margin of safety is applied in current reactor siting practice.

Experimental and analytical programs directed at providing a better understanding of the release and the subsequent transport of radioiodine following a loss-of-coolant accident were summarized. Programs that appear to have particular potential for identifying larger radioiodine attenuation factors than those currently applied in reactor siting practice are the following:

(a) Experimental and analytical studies directed at providing a quantitative understanding of the conversion of radioiodine to presistent species that exhibit long half lives in the containment atmosphere,

(b) Development of silver zeolite absorbers that will effectively retain both molecular iodine and presistent iodine species,

(c) Experimental and analytical studies directed at providing estimates of radioiodine retention by interior fuel pin surfaces, reactor system surfaces, and water within the reactor system during the transport of radioiodine from the core to the containment.

(d) Analytical and experimental studies directed at providing a method for quantitatively estimating the fraction of the generated radioiodine that will migrate from the fuel to the plenum of the fuel pin during reactor operation.

References

1. Reactor Site Criteria, Title 10, Code of Federal Regulations, Part 100 (10-CFR-100), February 11, 1961.

2. J. J. DiNunno, et al., Calculation of Distance Factors for Power and Test Reactor Sites, TID-14844 (March 1962).

3. D. H. Walker and W. A. Yuill, Fission Product Behavior Analytical Development Program, IN-1380 (June 1970).

4. D. H. Walker and G. W. Parker, Fission Product Behavior Experimental Program, IN-1381 (June 1970).

5. W. B. Cottrell (ed.), Nuclear Safety Program Annual Progress Report for period ending December 31, 1969, ORNL-4511 (March 1970).

6. J. Dugone, et al., LOFT Integral Test Program, IDO-17258K (April 1969).

7. Hypoiodous Acid. "An Airborne Inorganic Iodine Species in Steam Air Mixtures", J. H. Keller, F. A. Duce, D. T. Pence, and W. J. Maeck, paper presented at 11th AEC Air Cleaning Conference, August 31 - September 3, 1970.

8. "A Selective Adsorbent Sampling System for Differentiating Airborne Iodine Species" by J. H. Keller, F. A. Duce, and W. J. Maeck, paper presented at 11th AEC Air Cleaning Conference, August 31 - September 3, 1970.

9. "Application of Metal Zeolites to Radioiodine Air Cleaning Problems", by W. J. Maeck and D. T. Pence, paper presented at 11th AEC Air Cleaning Conference, August 31 - September 3, 1970.

10. The Staff of Battelle Northwest Laboratory, Nuclear Safety Quarterly Report for November, December 1969 and January 1970, BNWL-1315-1 (March 1970) p 2.1-2.13.

DISCUSSION

BEATTIE: I would like to ask if you have considered the question of probability, because as you know we are very interested in probability methods and their use in the safety branch of the UKAEA? I noticed on the diagram a very large spread depending on whether or not one assumes a given safeguard device worked or did not work. For example, the reactor contains up to 10^8 curies of I^{131} but the release at the end of the chain on the right hand side of the diagram can vary from one to about 2×10^4 curies I^{131}. Would you comment, Dr. Walker, on how you view your chances on eventually getting enough information to apply probabilities to these different lines?

WALKER: First to the probability question. It is not current practice in this country to apply the probability approach in reactor siting. We have done some work with that approach internally within our particular group and I would be happy to talk to you about that. We have attempted to identify the probability that the conservative attention now assigned to each of the processes will actually occur and that has proven quite interesting to us. We have also attempted to put together some probability estimates around the estimated releases of Loft reactor experiments which Idaho Nuclear is conducting, but we have not published these as yet. Secondly, relative to the difference between one and 10^4 curies. We feel that certainly it's potentially attainable within the technology of the next three or four years to identify that releases are as low as 10 curies. I do feel however that some additional margin of safety beyond that kind of a number (10 curies) would need to be applied in reactor siting considerations.

COMPARISONS OF AEROSOL EXPERIMENTS WITH A MODEL USED IN REACTOR SITING EVALUATION*

M. Greenfield
R. Koontz
R. Johnson
H. Morewitz

Atomics International,
A Division of North American Rockwell Corporation
Canoga Park, California

ABSTRACT

The theoretical basis of the HAA-3 aerosol agglomeration code is described. The code solutions have been compared successfully against sodium oxide aerosol experiments in two test chambers which differ by a factor of 50 in volume ratio. Since the large vessel is approximately the height of the primary vaults of a typical Liquid Metal Fast Breeder Reactor (LMFBR), HAA-3 can be confidently used in the evaluation of potential aerosol releases from hypothetical LMFBR accidents. The application of HAA-3 to LMFBR containment studies is discussed.

I. INTRODUCTION

In order to evaluate proposed sites for Liquid Metal Fast Breeder Reactors (LMFBR), and establish the capability of containment-related design features, various hypothetical accidents which release radioactive aerosols to the environment have been postulated. It is therefore necessary to study the transport of aerosols produced during sodium fires and other postulated LMFBR accidents involving the release of sodium, sodium oxide, fuel, and fission product particulates.

This paper first presents a comparison of the HAA-3 computer code solution of the general equation of aerosol agglomeration and data from various experiments on sodium oxide aerosols performed at high-particle concentrations in test vessels up to 30 ft in height (the approximate height of primary vaults for a typical LMFBR). The HAA-3 code is then used to calculate aerosol attenuation factors for typical LMFBR containment systems.

II. THEORETICAL MODEL

The behavior of a heterogeneous population of particles undergoing coagulation has been studied by a number of investigators. The theoretical formulation of the problem is usually given in the form of a general nonlinear integro-differential equation.[1-6] Solutions to this rather complex equation have been obtained by using computer codes.[7-12]

*Work performed under USAEC Contract AT(04-3)-701.

More recently,[13] the general equation has been modified to provide an analytical approach to describe the behavior of aerosols in a closed vessel. As modified, the complete equation* is:

$$\frac{\partial n(v,t)}{\partial t} = \frac{1}{2}\int_0^v n(v',t)n(v-v',t)F(v',v-v')dv'$$

$$- n(v,t)\int_0^\infty n(v',t)F(v,v')dv' - R(v)n(v,t) + S(v,t) \quad , \qquad \ldots(1)$$

where:

$v = r^3$ (i.e., spherical particles are assumed)

r = particle radius

$F(v,v')$ = normalized collision kernel which gives the probability of collision between two particles of radii, r and r', due to Brownian motion and due to differences in setting velocities (gravity)[14]

$R(v)$ = removal rate due to settling, wall plating, and leakage

$S(v,t)$ = source rate for particles of radius, r.

The first integral represents the rate of production of particles of size, v, due to all collisions between two particles of size, v' and $v - v'$. The second integral gives the rate at which particles of size, v, grow to larger sizes due to collisions with particles of size, v'.

The removal rate, $R(v)$, is given by

$$R(v) = G_R v^{2/3}\left[1 + C_1(v)\right] + P_R v^{-1/3}\left[1 + C_1(v)\right] + R_L \quad , \qquad \ldots(2)$$

where:

$G_R = 2g\delta/9h\eta$, the settling constant

h = height of chamber, $h = V_c/A_F$

η = viscosity

δ = density of aerosol material

g = acceleration due to gravity

$P_R = kTA_w/6\pi\eta\Delta V_c$, the plating constant

A_F = area of the floor

A_w = area of surface for plating

V_c = volume of chamber

Δ = distance, perpendicular to the wall, over which a gradient of the particle density is assumed to exist (Δ is an adjustable parameter, required to fit experimental wall plating data)

*For more complete details, see Reference 13.

K = Boltzman's constant

T = temperature.

The term containing G_R is the removal rate due to settling; the term containing P_R is the removal rate due to plating. The R_L term is the removal rate due to leakage and is a constant, independent of particle size. Both G_R and P_R are geometry dependent.

It is clear, from the structure of the terms in Equation 1, that the competing removal terms will be sensitive to the geometry, the chamber height, and relative values of the wall and floor areas. Further, the height of the chamber affects the time scale, and therefore the median particle size. A larger chamber means more time for agglomeration and, as a consequence, larger median sizes. This, in turn, affects the ratio of particle mass settled vs that plated. A large chamber should have a greater fraction of the mass appear as the settled component. Laboratories using liter-sized vessels, cubic meter sizes, or very large chambers should expect entirely different dynamic results.

Straightforward numerical solution[12] of the coagulation equation (Program HAA-2) has proved very valuable, but requires excessive computing times for concentrations $>4\ \mu g/cm^3$. Interest in extending the calculations to higher concentrations has therefore led to the development of an approximate method of solving the equation.

The solution of Equation 1 has been developed[15] by assuming that a log-normal distribution is maintained throughout the life of the aerosol. The integro-differential equation is replaced by three simultaneous, first-order differential equations, in which the dependence on v has been removed. In order to do this, the form of the distribution must be assumed. Since both experiment and calculation (Program HAA-2) have indicated that the distribution of particles is very nearly log-normal,[12] that type of distribution has been used. The formal expression for the log-normal distribution function is

$$n(v,t)\,dv = \frac{N(t)}{\sqrt{2\pi u(t)}} \exp\left\{-\frac{\left[\ell n \frac{v}{V(t)}\right]^2}{2u(t)}\right\}\frac{dv}{v} \quad , \qquad \ldots(3)$$

where:

N(t) = total concentration of suspended particles (all sizes)

V(t) = logarithmic mean volume of a particle times $3/4\pi$

u(t) = logarithmic variance.

By using $\mu(t) = \ell n\, V(t)$ and $S = \ell n\, v$, the volume moments times $(3/4\pi)^k$,

$$X_k(t) = \int_o^\infty n(v,t) v^k dv$$

may be evaluated; thus,

$$X_k(t) = N(t) \exp\left[k\mu(t) + \frac{1}{2} k^2 u(t)\right] \quad \ldots (4)$$

In particular, the three moments are:

$$X_0(t) = N(t),$$

$$X_1(t) = N(t) \exp[\mu(t) + (1/2)u(t)],$$

and $$X_2(t) = N(t) \exp[2\mu(t) + 2u(t)].$$

In fact, the moment $X_0(t)$ is just the total number of particles, and hence identical with the parameter $N(t)$ already introduced. The moment $X_1(t)$ is just the total volume contained in the aerosol particles, and has the convenient property of being unaffected by coagulation. Both these moments, however, are relatively accessible to experimental determination. On the other hand, the higher moments are the ones most sensitive to the low-probability "tails" of the distribution, where the log-normal approximation is likely to be least satisfactory. In view of these considerations, the choice of moments is not really arbitrary. $X_2(t)$ is the distribution of the volume of the particles.

The basic assumption in the approximate solution to the integro-differential equation for the behavior of an heterogeneous aerosol was that the aerosol distribution remained log-normal. This assumption is good, as long as agglomeration is an important process. However, as the number concentration decreases with time, a point is reached at which the agglomeration process becomes negligible. In the vicinity of this point, the approximate solution becomes incorrect. If the behavior of the aerosol is to be calculated beyond this point, a more suitable approximation must be used. To accommodate this problem, the approximate solution is used in the HAA-3 program until the ratio of the agglomeration rate to the settling rate reaches an input value, where the agglomeration rate is equal to or less than the settling rate. At this point, the method of calculation is changed; a stirred settling model, SSM,[17] is used. In this model, the agglomeration processes are neglected. Only settling and leakage are considered, and the log-normal assumption is no longer required.

There is a separate SSM code available, which can be used to calculate the size distributions of the airborne mass fraction and of the leaked mass fraction, as well as the airborne mass, leaked mass, and settled mass fractions. This code, SMM-5,[18] computes particle size distributions by dividing the size range into 30 intervals, and performing the Gaussian quadrature separately on each interval. The distributions calculated at selected times are printed and plotted at the completion of the calculations. If distributions are desired after the agglomeration rate is negligible, the SSM-5 code must be used instead of the SSM version in the HAA-3 program. This may easily be done by inputting into the SSM-5 code the log-normal distribution parameters calculated by HAA-3 at the time when the calculation switches to SSM.

III. EXPERIMENTS

Aerosol experiments have been performed in two vessels, the LTC* and LTV, which have both been described previously.[19,20]

Large Test Vessel

The Large Test Vessel (LTV) is a 10-ft diameter by 30-ft high, 2200 ft^3 cylindrical pressure vessel, rated at 40 psig and mounted vertically within a building. The entire vessel is covered with 2 in. of high-temperature insulation. (See Figure 1.) Vessel penetrations include instrument bulkheads, to allow penetrations of instruments and power leads, experimental nozzles for aerosol sampling, 18-in. diameter manholes (2 each), three viewing windows, and an insulated fill line for dumping liquid sodium from an external preheat tank to the 2.45 ft by 2.45 ft (6 ft^2) burn pot.

LTV Instrumentation

Continuous measurements of temperature, oxygen, pressure, and particulate fallout (using recording balances) in the LTV vessel are recorded on a 300-channel (3-channels/sec) data logger.

Additional measurements are made to characterize the aerosol, such as wall and floor deposition vs time, concentration vs time, and particulate aerodynamic diameter vs time. Humidity is measured before and after each experiment.

The sampling devices for measuring aerosol concentration and size are attached to the front end of a long tube which passes through a ball valve and O-ring seal. The samplers are thus placed directly into the vessel atmosphere during the sampling period, eliminating settling when one samples particulates through a tube. The aerosol is collected on a membrane-type of filter paper for determining concentration. The aerodynamic size of the aerosol is determined from an 8-stage, 3-hole/stage impactor. Sample positions are located at three different heights.

LTV Measurements

Figure 2 is a schematic representation of the LTV, indicating the locations of the various collection devices, sampling ports, and the burn pan. Sodium is heated to temperatures of the order of 900 to 1200°F. The sodium reacts with the oxygen, releasing a fraction of the reaction products into the vessel. To provide convective air currents to produce a stirred aerosol environment, the sodium burn pan is heated for the time of interest, during which samples are collected. Measurements are made of five independent quantities, as a function of time: (1) suspended mass concentration, C, (2) mass settled on the floor, M_F, (3) mass plated on walls, M_W, (4) median radius by volume (or mass), $\bar{r}_v$, and (5) the geometric standard deviation, σ, of the particle size distribution.

*The Laboratory Test Chamber (LTC) is a 40 ft^3, 6-ft high, cylindrical vessel, in which previously reported experiments on both Na_2O[21] and UO_2[22] aerosols have been performed.

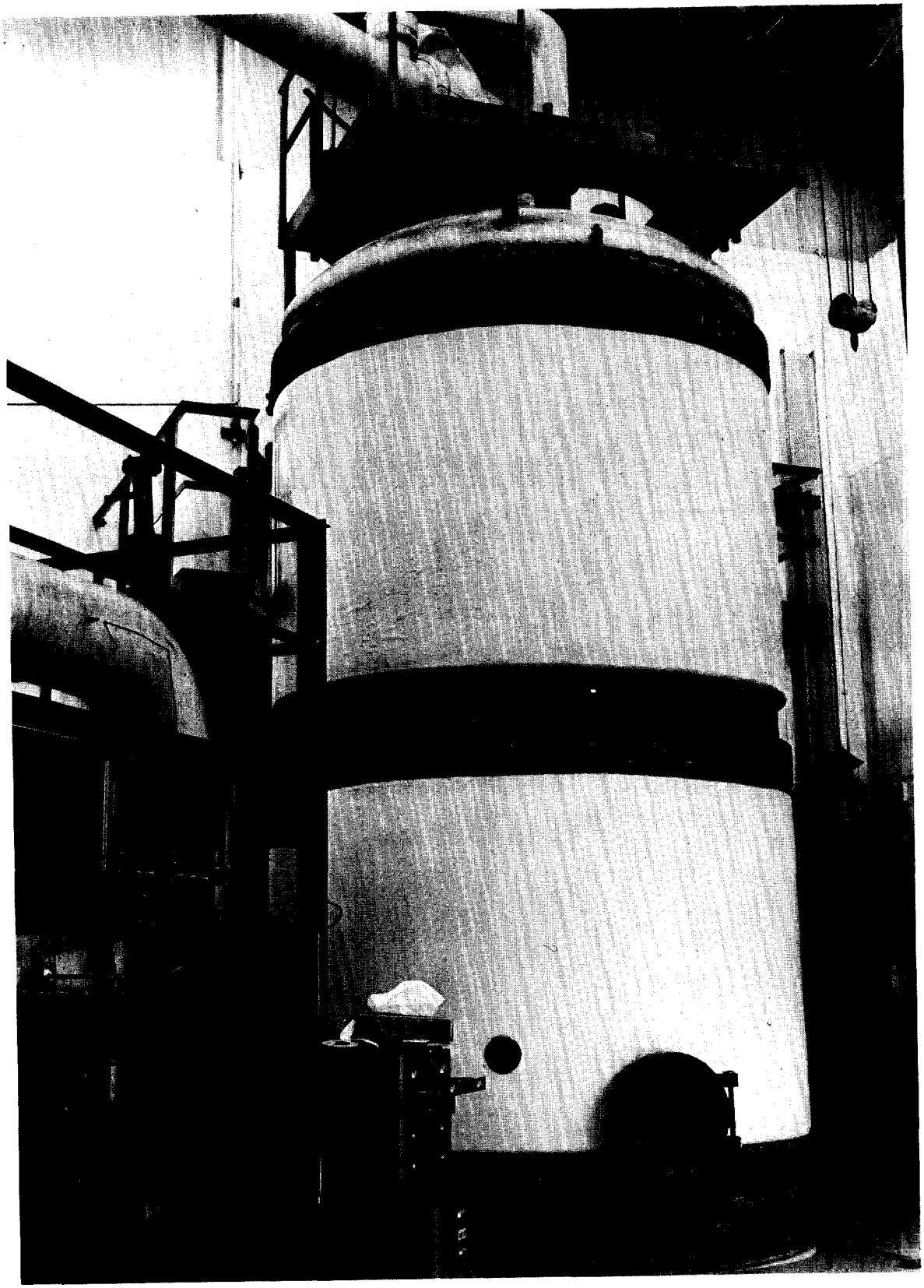

00-102207

Figure 1. Large Test Vessel

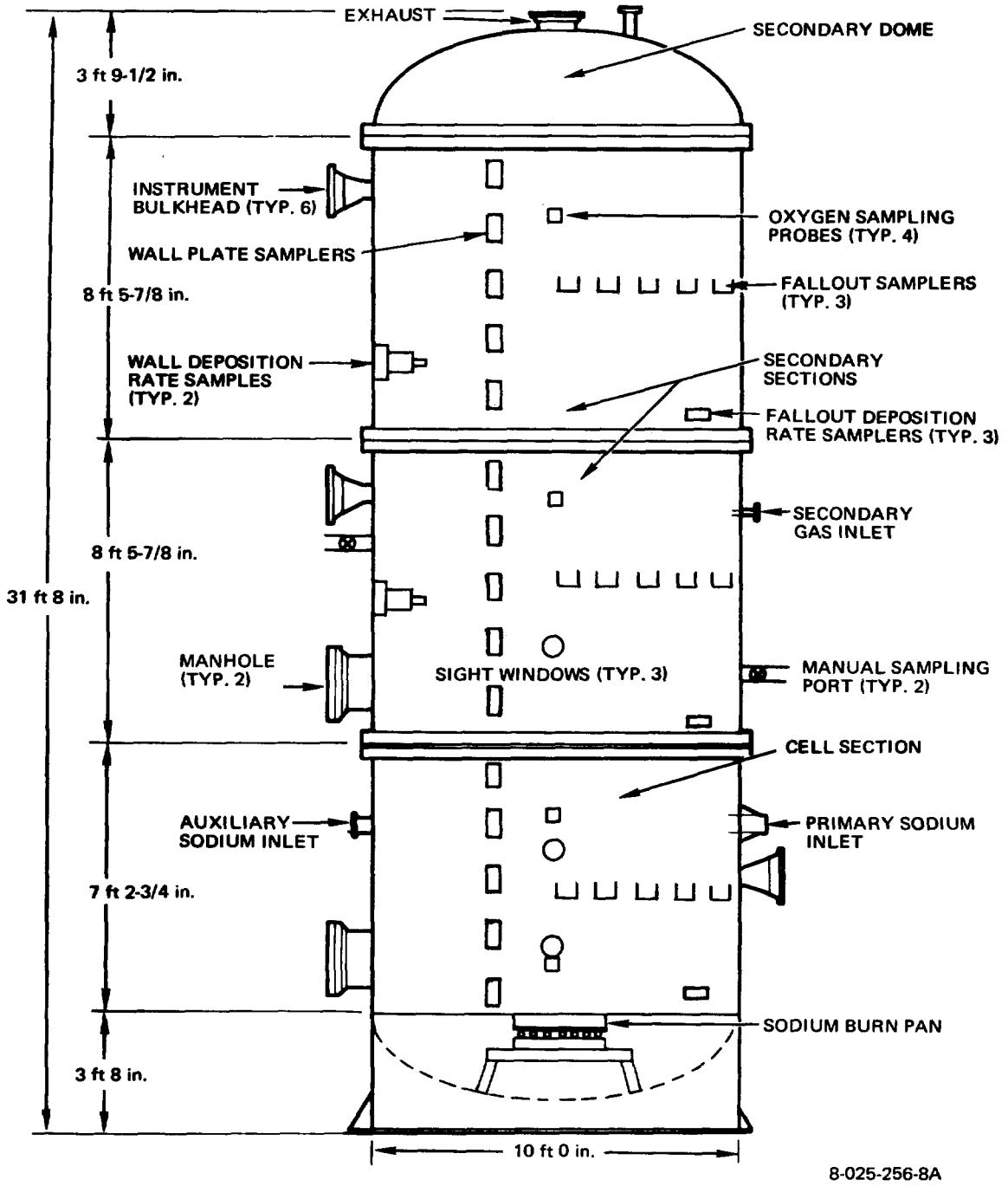

Figure 2. Large Test Vessel Sampler Positions

The aerosol collected on a membrane filter paper yields the suspended mass concentration as a function of time. The turntable data permits computation of the settled mass as a function of time. The data from the metal strips leads to the computation of the mass deposited on the wall as a function of time. The mass released as a function of time is computed on the basis of measurements of the oxygen consumption rate and the ratio of total mass released to mass burned. The total mass released is checked for mass balance by comparisons with the total mass settled on the floor, and the total mass deposited on the walls (obtained by complete washdown of the vessel at the conclusion of the experiment). Another method used to obtain total mass released as a function of time is to add three components: (1) mass suspended, (2) mass settled (turntable data), and (3) mass deposited on the wall (strip data). The two independent methods of measuring total released mass as a function of time are reasonably consistent. The burn time is characterized by the oxygen consumption rate.

IV. COMPARISON OF EXPERIMENT AND AEROSOL MODEL

Sodium burning experiments in the LTV were performed with released mass concentrations as high as 175 $\mu g/cm^3$ as oxide ($\sim$130 $\mu g/cm^3$ as sodium). The observed increases in median radius by volume were of the order of 4 to 5 μm, some 8 to 10 times as large as the measured initial size of 1/2 μm. For modeling these experiments, it is assumed that the material density of the oxide is effectively 25% of the ideal (2.27 g/cm^3 for Na_2O, and 2.7 g/cm^3 for Na_2O_2). This assumption is based on work reported by Lane and Stone[23] on the effective density or shape factor (SF), reached by agglomerated particles that are not closely approximated as spheres, with looser packing and a greater percentage of voids. They found such particles reaching a stable percentage of $\sim$25% of the unit particle density (i.e., SF = 1/4) when the effective diameter is $\sim$5 times the unit particle size.

Figures 3 through 9 give the detailed LTV test results for the observables as a function of time, for Tests 3, 4, and 5. The mass released, M_R, is given in Figure 3 for Test 3. The mass settled is given in Figure 4 for Test 4. The airborne mass concentrations are given in Figures 5, 6, and 7 for Test 3, 4, and 5. The airborne mass concentration for later times (followed for 4 to 5 decades of concentration reduction) is given in Figure 8 for Test 3. The median radius by volume is given in Figure 9 for Test 5.

Similar test results[21] for LTC Test No. 14 are given in Figures 10 and 11. Figure 10 shows the sodium oxide concentration in the air as a function of time, while Figure 11 shows the cumulative mass plated on the LTC wall and floor as a function of time. Computer solutions of Equation 1, obtained by means of the HAA-3 code, are shown, along with the experimental findings.

The ability to compare theory and experiment to the high concentration of sodium oxide released to the vessel atmospheres was due to the previously discussed modification of the method used to solve the general equation. The input parameters for the HAA-3 code are given in Table 1.

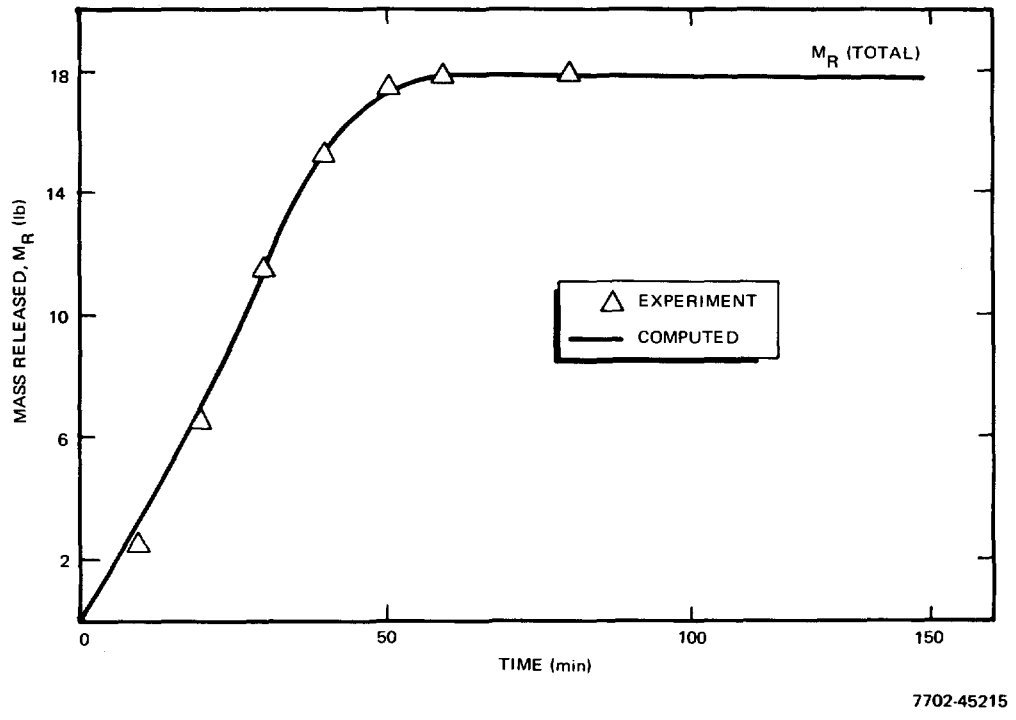

Figure 3. Mass Released for Test No. 3

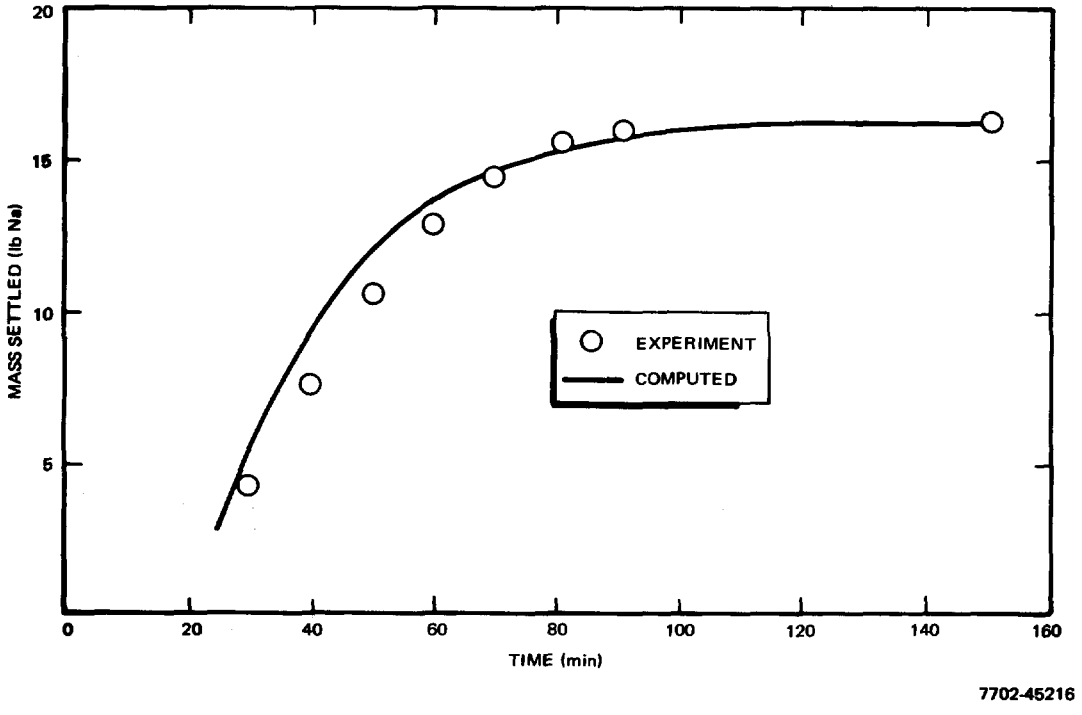

Figure 4. Mass Settled for Test No. 4

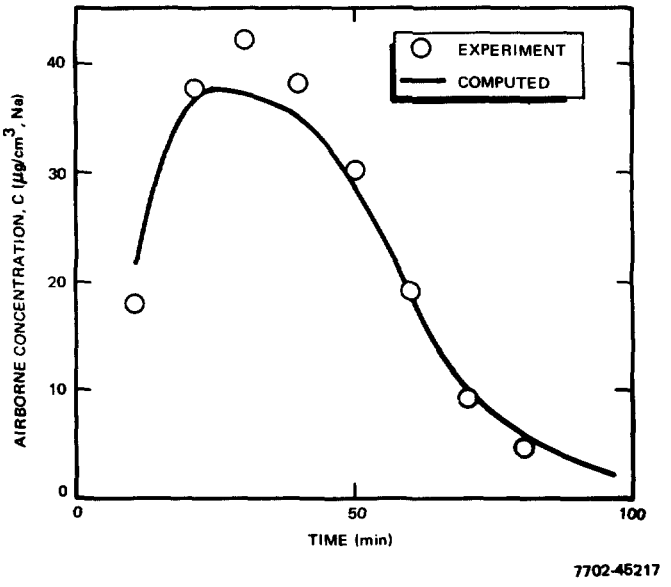

Figure 5. Airborne Mass Concentration for Test No. 3

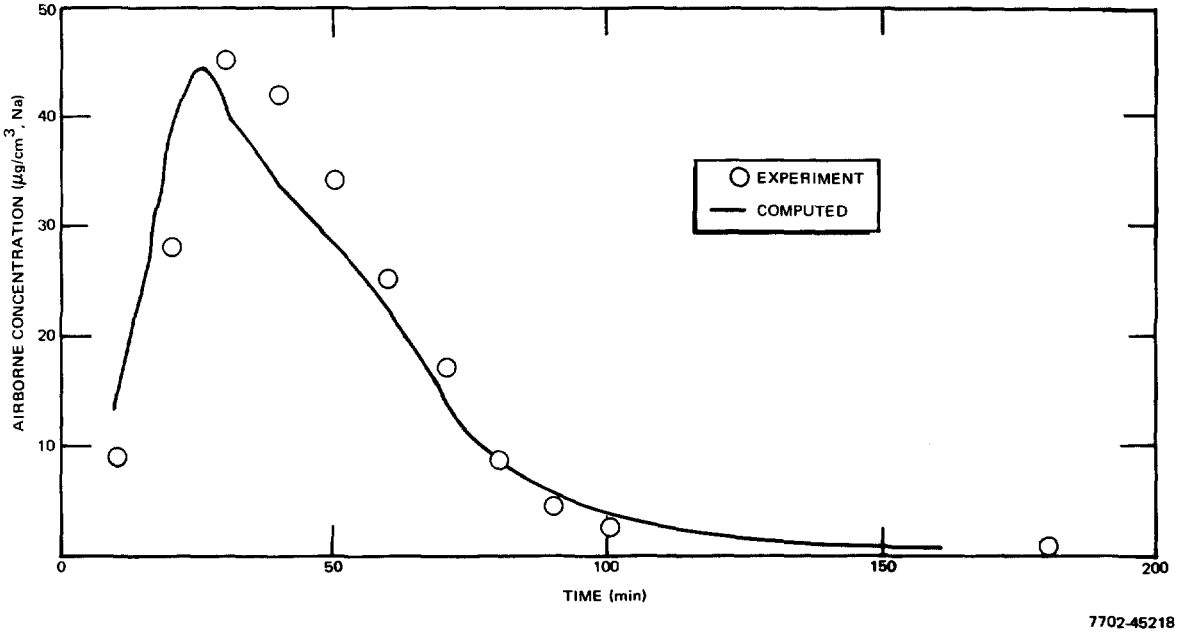

Figure 6. Airborne Mass Concentration for Test No. 4

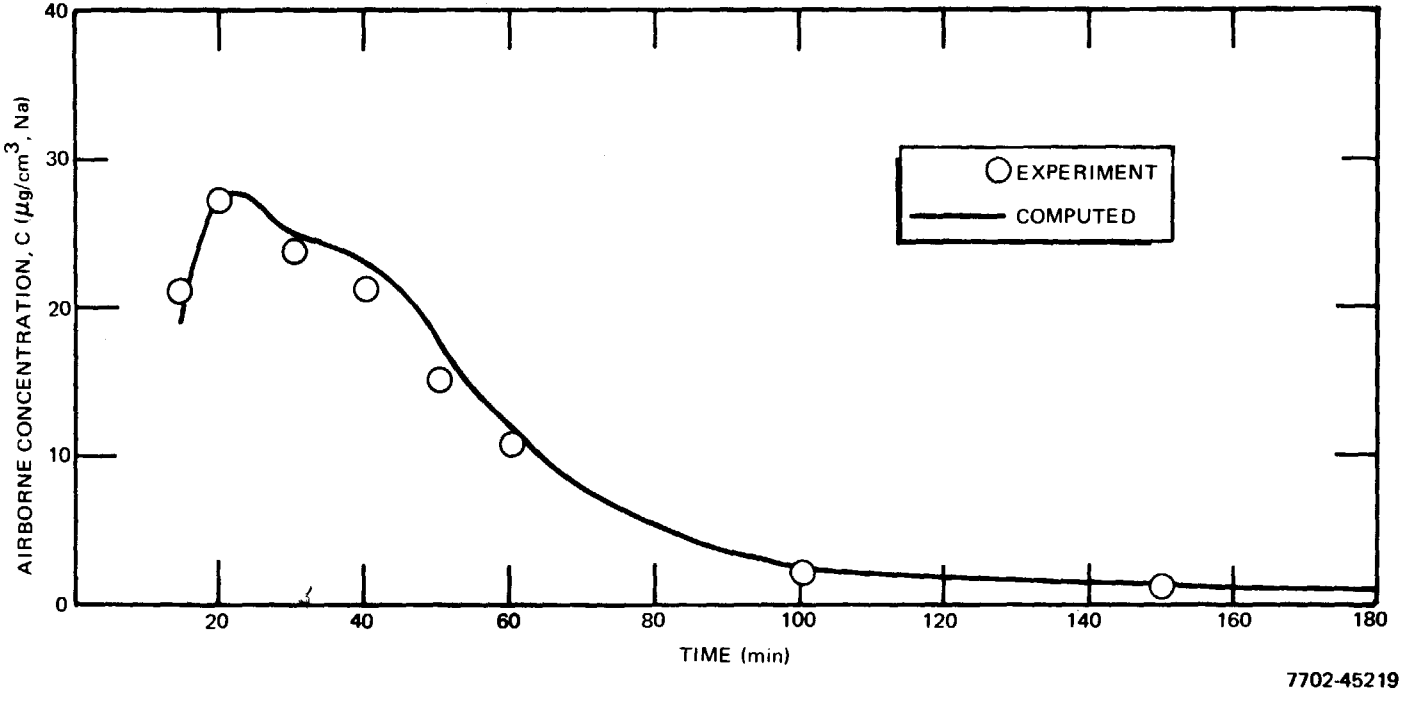

Figure 7. Airborne Mass Concentration for Test No. 5

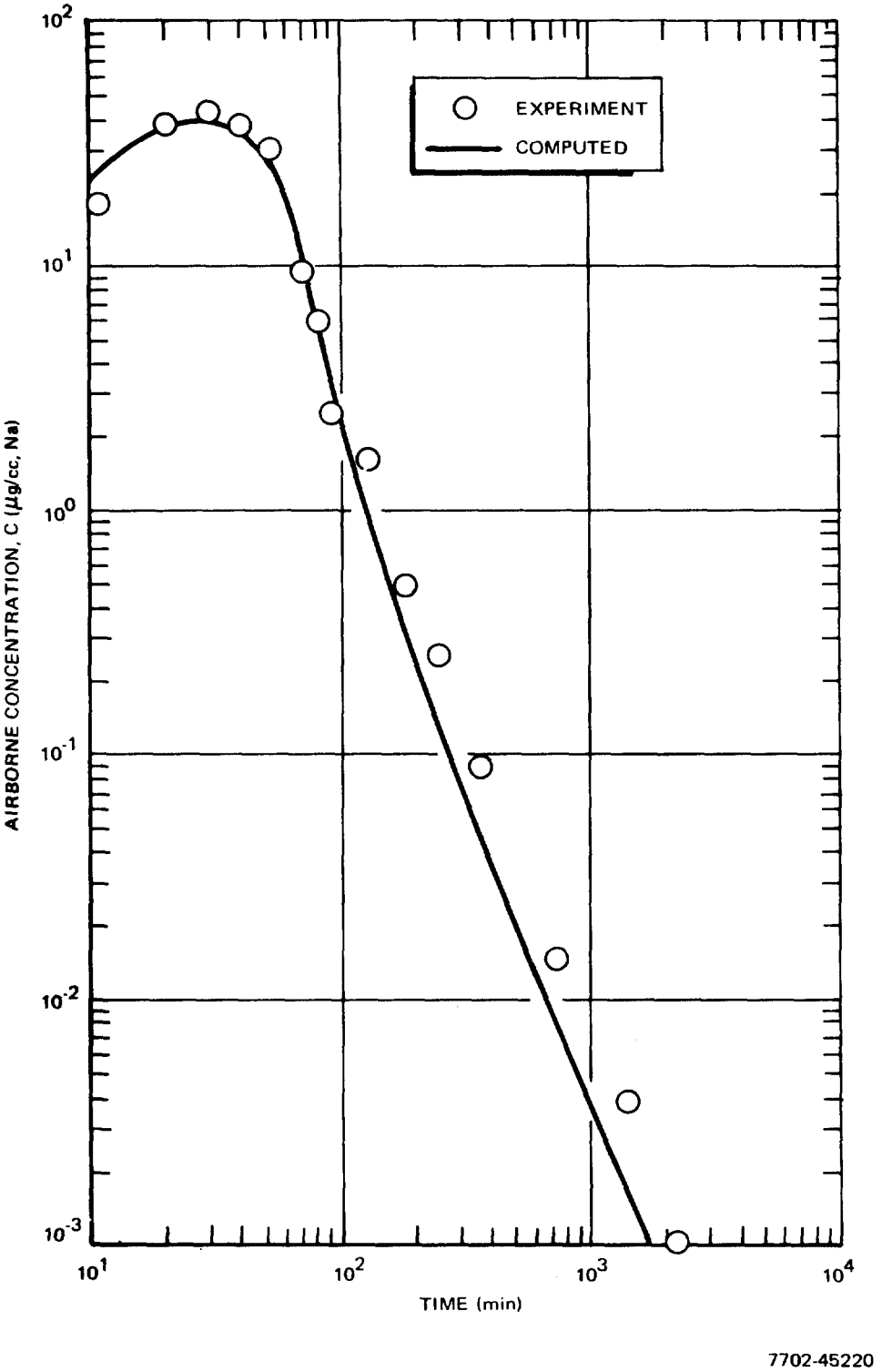

Figure 8. Airborne Mass Concentration at Extended Time for Test No. 3

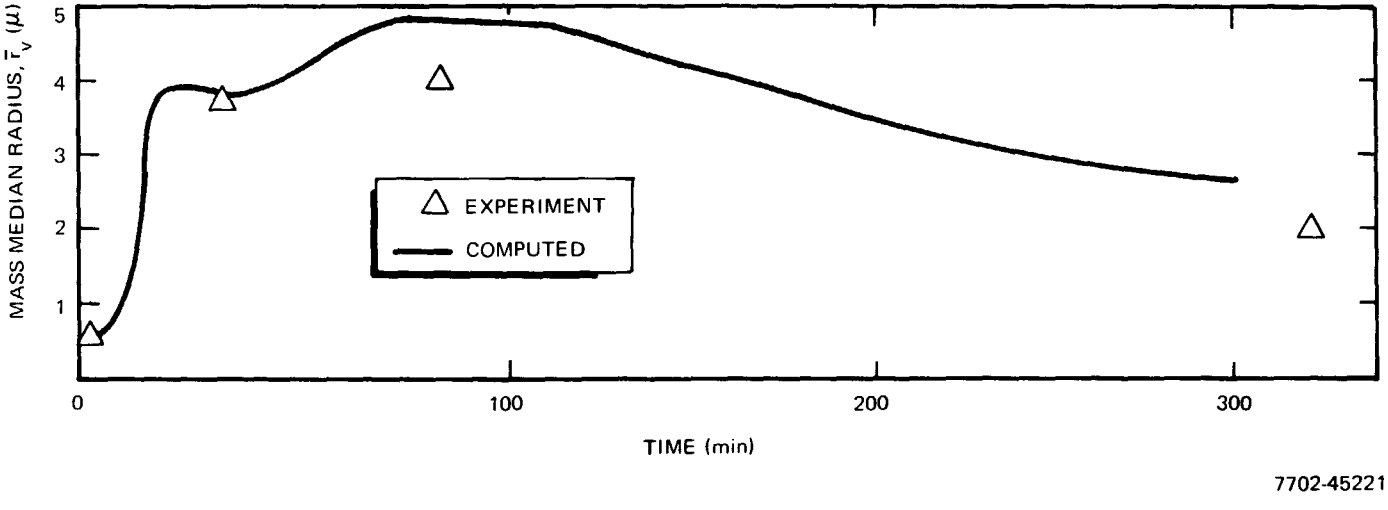

Figure 9. Airborne Particle Size for Test No. 5

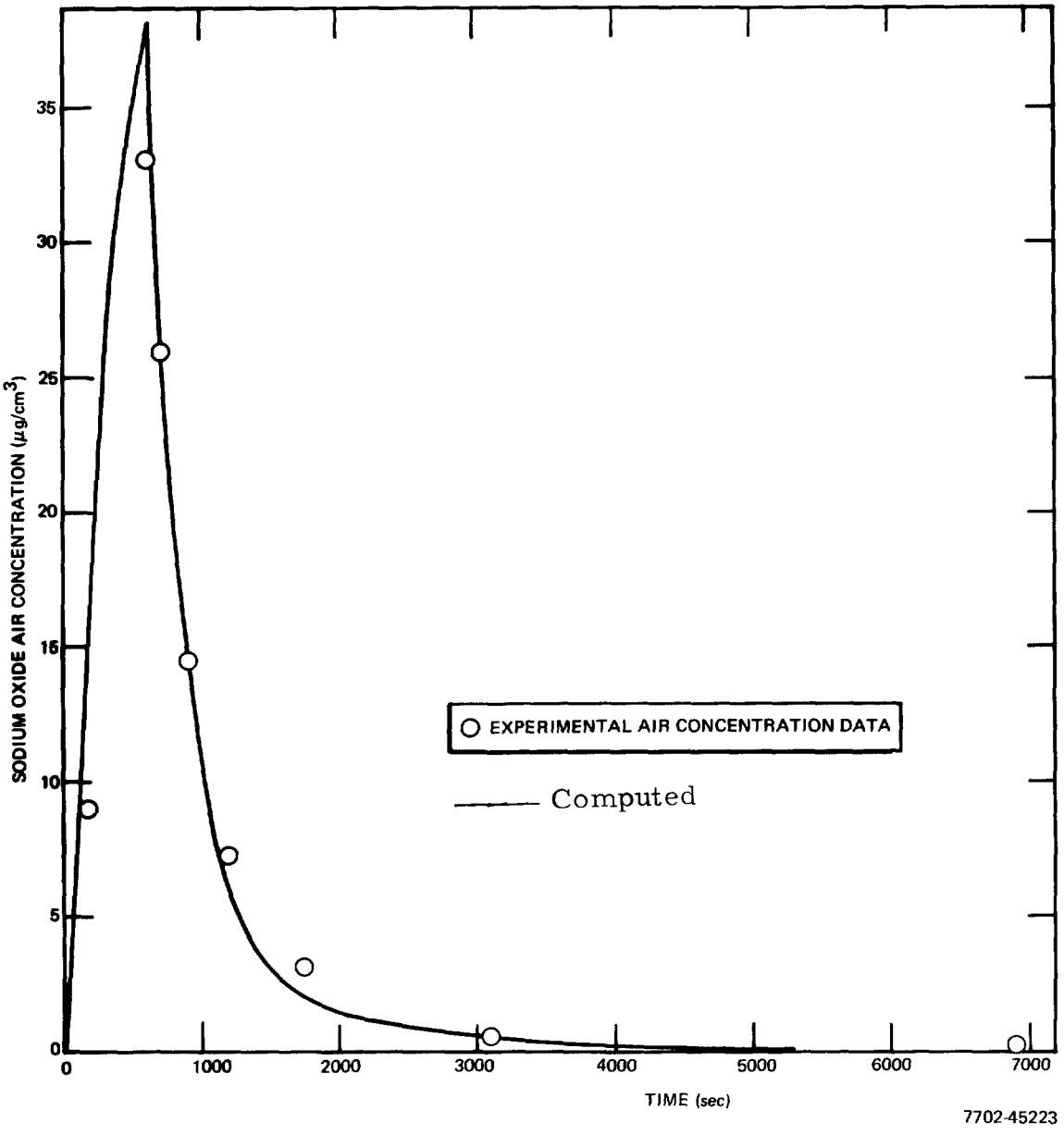

Figure 10. Comparison of HAA-3 to LTC No. 14 — Sodium Oxide Concentration in Air

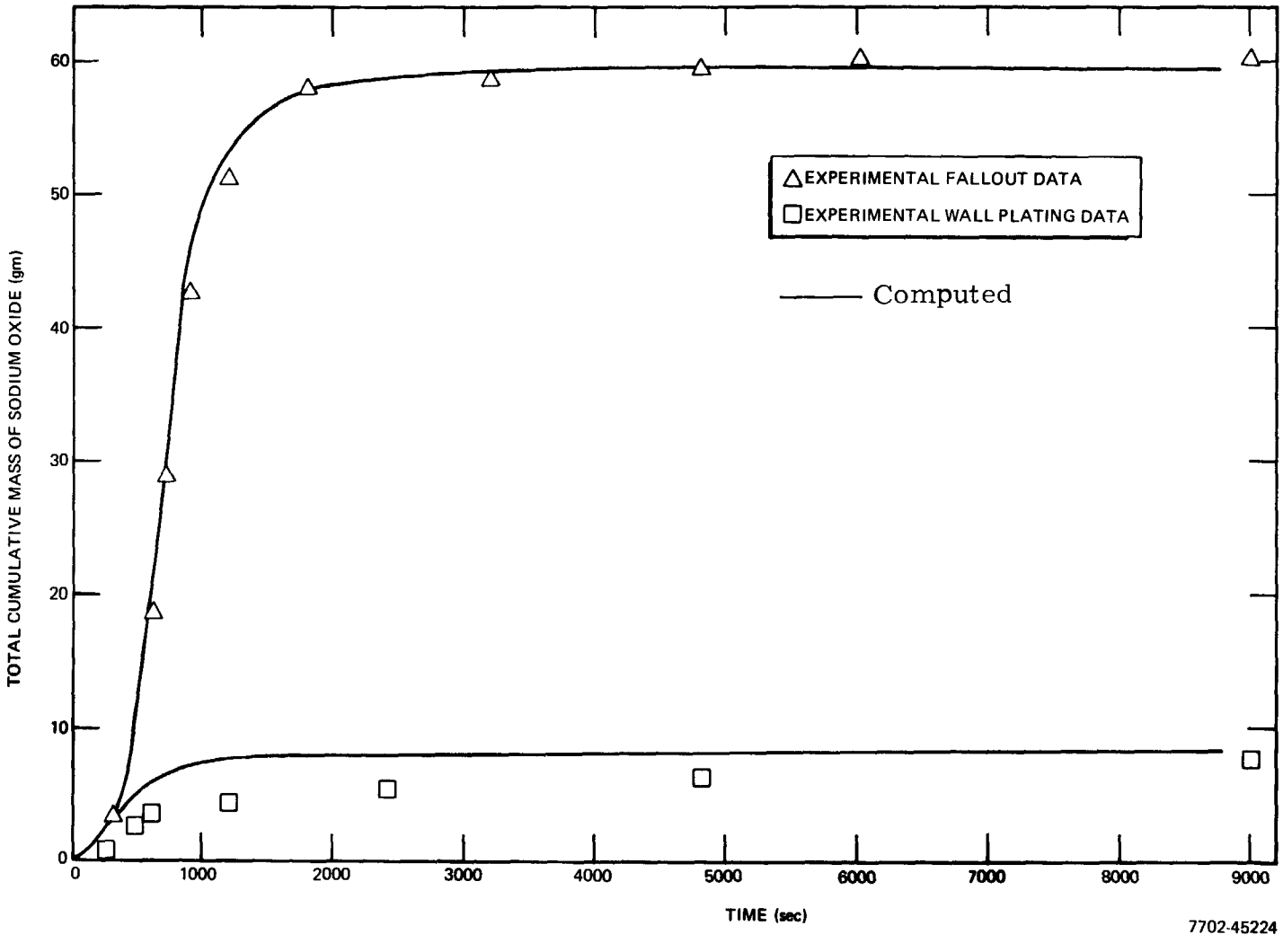

Figure 11. Comparison of HAA-3 to LTC No. 14 – Cumulative Mass Plated on Wall and Floor

Note that M_R, the released mass; C_R, the released mass expressed as a concentration (i.e., M_R/V); τ, the burn time; $Q = C_R/\rho_{effective}$, the fraction of space occupied by the released mass; $\bar{r}_v(t = 0)$ and σ, the parameters describing the initial particle distribution; are all measured quantities. The shape factor or effective fraction of unit particle density, called SF, equals 1/4, and was discussed previously. N_o, the initial particle concentration; and S_o, the source term, N_o/τ; are computed from the previous quantities. Also employed as code input is the measured, released mass as a function of time, as given in Figure 3. The computed results are given as the solid curves in Figures 3 through 11.

What is noteworthy is the simultaneous fitting of theory to four sets of data for each experiment. There are no adjustable constants, and only one adjustable parameter (wall plating distance, Δ). A further significant test of the model represented by Equation 1 is its use in the comparisons with experiments performed both with high and low initial concentrations, and in small and large test vessels, so that geometrical factors would be changed over a wide range.

This portion of the paper has given comparisons of theory and experiment for a very different geometry than previously studied[13] (volume ratio exceeds 50). Also, the released mass differs, by a factor of 50, between the LTC and LTV. The ability of the theory to accommodate these large differences in mass concentration and geometry is a strong indicator of the basic validity of the theory. In particular, the correct prediction of the dramatic increase in particle size in the LTV experiments has a most important implication for safety, since large sizes, which result from large released masses, mean rapid fallout will occur in the primary containment.

TABLE 1
CODE INPUT PARAMETER VALUES FOR SODIUM OXIDE AEROSOLS IN THE LTV AND LTC

Selected Input Parameter to Simulate	LTV Test				LTC Test
	3	4	5	6	14
M_R (gm Na)	8120	7800	3830	36	66
C_R ($\mu g/cm^3$ Na)	135	130	64	0.64	60
τ (sec)	3800	3200	4200	1200	600
$Q = C_R/\rho_{effective}$ (μ^3/cm^3)	8×10^7	7.68×10^7	3.86×10^7	6.17×10^5	3.62×10^7
$\bar{r}_v(t = 0)$ (μ)	0.5	0.5	0.5	0.5	0.5
σ	2	2	2	2	2
SF	1/4	1/4	1/4	1.0	1/4
N_o (oxide particles/cm^3)	1.3×10^9	1.3×10^9	6.4×10^8	10^7	5.8×10^8
S_o (particles/cm^3-sec)	Variable	Variable	Variable	Variable	Variable
Δ (wall plating parameter) (μ)	1×10^{-5}	2×10^{-5}	2×10^{-5}	5×10^{-4}	2×10^{-5}

V. APPLICATION OF HAA-3 TO LMFBR SITING STUDIES

The HAA-3 model has been shown to agree well with experimental data in a vessel 30 ft in height, and thus it can be confidently used for LMFBR reactor siting studies.

From these studies, the amount of material which could leak to the environment can be shown to be dependent on the amount of material released in the primary vault during the LMFBR Design Basis Accident (DBA), the behavior of the resulting aerosol in both primary and secondary containment (double containment) or in the single containment structure, and the leakage characteristics of the containment structures.

Parametric studies have been performed with the HAA-3 model to evaluate the effects of airborne concentrations up to 200 $\mu g/cm^3$ in large containment volumes. Calculations were performed for various instantaneous releases of an aerosol with a density of 2.27 gm/cm^3 and an initial mass median particle size of 0.5 μ with log-normal standard deviation of 2.0. The times for the initial concentration to decrease to one-half its original value are shown in Figure 12. As the concentration is increased, the rate at which the material settles to the floor is increased. Since the fraction of the airborne material which can leak is a function of the concentration, the faster the air concentration is decreased by settling, the lower the fraction which can escape. Figure 12 also shows that, at high concentrations, the taller the building, the faster the concentration decreases.

Table 2 compares the total masses leaked for monosized and heterogeneous particle size distributions. For these calculations, the volume of the inner vault (typical of an LMFBR design) was 1.5×10^5 ft^3, the height was 30 ft, and the leak rate was constant at 10 vol %/day. If the input material is monosized ($\sigma = 1.0$), changes in the initial size of the aerosol do not change the leaked mass significantly, for initial concentrations >200 $\mu g/cm^3$. For heterogeneous aerosols ($\sigma = 2.0$), the mass leaked is inversely proportional to the initial median size. A lower initial concentration results in more total leaked mass, because agglomeration is less effective at lower concentrations. The air concentration does not decrease as rapidly, and thus more material can leak in a given time.

Calculations have been made, using the model, to evaluate the effect of double containment on the mass leaked to the atmosphere. For these calculations, the inner containment volumes were either 1.6×10^4 or 1.97×10^4 ft^3, and the outer containment volumes were 2.7×10^6 and 3.34×10^6 ft^3. The design leak rate for the inner containment was 10 vol %/day at 30 psig, and the outer was 1 vol %/day at 15 psig. Because of heat transfer from the gas to the containment walls, the pressures decayed, so that the leak rate was not constant. The results in Table 3 show that, as the air concentration in the inner containment volume is increased, the fraction of material, originally released in the inner volume, which can leak to the atmosphere is decreased.

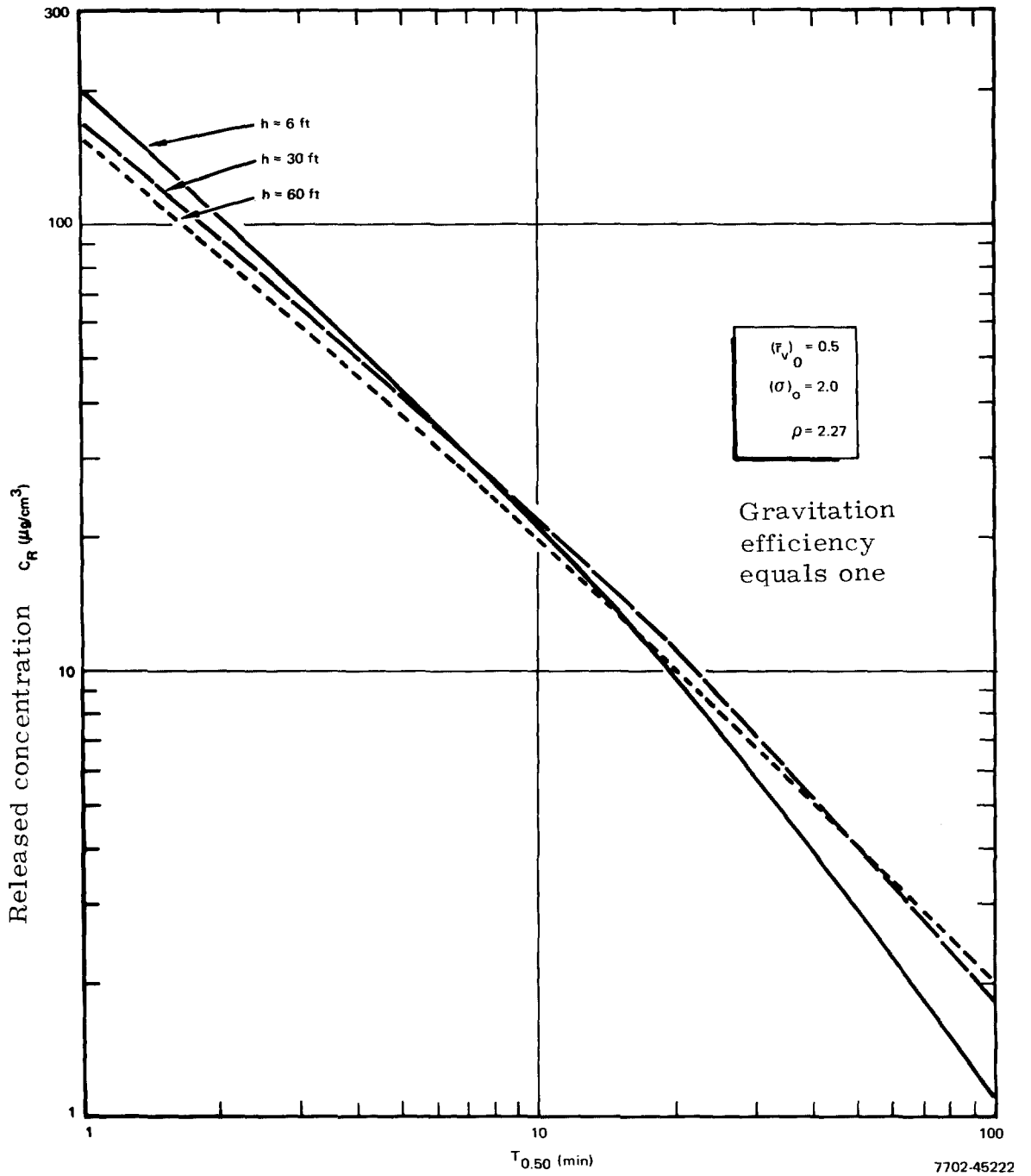

Figure 12. Time for C/C_o to Reach 50% as Function of Chamber Height

TABLE 2

EFFECTS OF INPUT PARTICLE SIZE PARAMETERS

Concentration ($\mu g/cm^3$)	$(\bar{r}_v)_0$	$(\sigma)_0$	ρ	Initial Air Concentration Half Time (sec)	Total Mass Leaked From Inner Containment (gm)
235	0.1	1.01	1.0	62.0	73.8
235	0.5	1.01	1.0	61.5	73.4
235	1.0	1.01	1.0	56.5	67.6
235	0.1	2.00	1.0	62.5	74.7
235	0.5	2.00	1.0	40.0	48.0
235	1.0	2.00	1.0	27.1	33.5
23.5	0.1	1.01	1.0	608	84.8
23.5	0.5	1.01	1.0	603	83.7
23.5	0.1	2.00	1.0	607	86.2
23.5	0.5	2.00	1.0	400	63.3
23.5	1.0	2.00	1.0	282	51.1

TABLE 3

MASS FRACTION LEAKED TO ATMOSPHERE

Mass Released to Inner (kg)	Inner Volume Air Concentration ($\mu g/cm^3$)	Fraction Leaked to Atmosphere
419.5	75	8.9×10^{-7}
419.5	92	7.5×10^{-7}
1031	185	4.0×10^{-7}
1031	226	2.5×10^{-7}
1287	230	2.5×10^{-7}
1287	282	2.4×10^{-7}

VI. CONCLUSIONS

A model which describes the coagulation and removal of aerosol particles by various mechanisms has been formulated. The model has been tested against a wide range of particulate concentrations in air in two chamber volumes which are in a volume proportion of 50:1. For each experiment, the fit of the computed data to four time-dependent sets of experimental data is good. As a result, the HAA-3 model can be confidently used in studies of aerosol transport following the DBA.

The model has been used to evaluate the mass leaked for various LMFBR hypothetical accident conditions in large containment volumes. It has been shown that the fraction of the released mass which can leak to the atmosphere is inversely proportional to the initial concentration. The calculations also show that, as the containment height is increased, the leaked mass will decrease for high concentrations in a stirred environment.

For typical LMFBR double containment calculations of hypothetical reactor accidents, using the HAA-3 aerosol model shows that reduction factors of 2×10^{-7} to 9×10^{-7} can be applied to the fuel - sodium - fission product material which would leak from the outer containment and create a hazard to the public. [This fact does not include the attentuation of the aerosol particulates in the leak path of the containment barriers.[24]]

REFERENCES

1. M. Smoluchowski, Vol 2, Physik. Chem. (Leipsig) 92, 129 (1917)
2. H. Muller, Kolloid, Beih. 26, 257 (1928)
3. H. Muller, Kolloid, Beih. 27, 223 (1928)
4. T. E. W. Schumman, Roy. Met. Soc. 66, 195 (1940)
5. D. E. Goldman, Handbook of Aerosols (Atomic Energy Commission, Washington, D. C., 1950) p 70
6. B. Friedman and M. Shiffman, Office of Technical Services PB 23710; also referred to as Applied Mathematics Panel Memo 100.1M, National Defense Research Committee (1944)
7. G. Zebel, Kolloid-Z., 156, 102 (1958)
8. S. K. Friedlander, J. Meteor., 17, 479 (1960)
9. D. L. Swift and S. K. Friedlander, J. Colloid Sci., 19, 621 (1964)
10. S. K. Friedlander and R. E. Pasceri, J. Atm. Sci., 22, 571 (1965)
11. G. M. Hidy and D. K. Lilly, J. Colloid Sci., 20, 867 (1965)
12. P. Spiegler, J. G. Morgan, M. A. Greenfield, and R. L. Koontz, NAA-SR-11997, Vol I (1967)
13. M. A. Greenfield, R. L. Koontz, and D. F. Hausknecht, "Comparison of Experiment With a General Equation for the Coagulation of Heterogeneous Aerosols," AI-AEC-12878 (1969)
14. P. G. Saffman and J. S. Turner, J. Fl. Mech. 1, 16 (1956)
15. E. R. Cohen and E. U. Vaughan, "Approximate Solution of the Equations for Aerosol Agglomeration," (to be published)
16. R. S. Hubner, "An Approximate Solution to the General Equation for the Coagulation of Heterogeneous Aerosols," AI-AEC-Memo-12880 (1969)
17. R. L. Koontz, R. S. Hubner, and M. A. Greenfield, "The Effect of Aerosol Agglomeration on the Reduction of the Radiological Source Term for the LMFBR Design Basis Accident," AI-AEC-12837 (1969)
18. R. S. Hubner, "SSM-5," (to be published)
19. R. P. Johnson, S. R. Price, and R. N. Cordy, "Description of the Sodium Fires Test Installation," AI-AEC-12759 (1969)
20. C. T. Nelson, L. Baurmash, and R. L. Koontz, Proc. 9th AEC Air Cleaning Conf., CONF-660904, 860 (1967)
21. R. L. Koontz, C. T. Nelson, and L. Baurmash, "Modeling Characteristics of Aerosols Generated During LMFBR Accidents," Treatment of Airborne Radioactive Wastes, Proc. of a Symposium, New York, August 26-30, 1968, IAEA, Vienna (1969)
22. L. Baurmash, C. T. Nelson, and R. L. Koontz, "The Characterization of UO_2 Aerosols by Aerodynamic Parameters," Treatment of Airborne Radioactive Wastes, Proc. of a Symposium, New York, August 26-30, 1968, IAEA, Vienna (1969)
23. W. R. Lane and B. R. D. Stone, International Conference on Mechanisms of Corrosion by Fuel Impurities, Butterworths (1963)
24. C. T. Nelson, J. Granger, R. L. Koontz, and L. Baurmash, "Measurement of Particle Filtration Efficiencies of Building Materials," Paper 11-1, this conference (1970)

BAKER: I wonder if you would care to comment on the possibility that the aerosols being leaked to the outside atmosphere might not be the same as that inside the containment. In other words, the possibility of having a pressurized aerosol can effect where the material that, as you assume in your model drops out and forever more is retained in the event of a leak on the bottom of the containment might become entrained and constitute an appreciable part of your external airborne source.

KOONTZ: I'm not sure I'm familiar with this effect, but it depends on whether you assume one leak path exists. For instance if the leak path does indeed exist in the bottom of the containment vessel in the present double containment system, I don't see how it could affect what gets into the secondary vessel at all. Since I didn't show a diagram of a typical vault secondary containment vessel, I can't answer that one at all. When this material leaks from the primary to the secondary, there is a considerable reduction in the concentration. The concentration will drop from 200 micrograms per cubic centimeter in the primary vessel to less than 1 microgram per cubic centimeter in the secondary vessel. This still represents a lot of mass when you multiply it times the volume. However, I don't see the lower concentration effecting the released quantity.

BAKER: Perhaps I can clarify what I mean. It is not an easy concept possibly. The reason that your airborne concentration in the secondary containment is so low is that the bulk of your material, according to your model, has settled out in the primary containment and is no longer available for leakage. What I'm saying is suppose that your leakage path is also where the fallout has become heaviest and the concentrations that you have calculated are now driving out, sweeping out, that which has already deposited in the primary vessel. Then would this not lead to a possible high concentration in the secondary vessel?

KOONTZ: I think you have to assume that some mechanism will cause the particle to rise (some force like turbulence, which would have to be considerable). Secondly, the pressure is forever decreasing in this primary vessel because of temperature losses. And pretty soon you don't have any driving force at all. One of the reasons that the leaked aerosol concentration decreases so low is because not only is it falling out, but the pressure (the leak rate) is decreasing also.

BEATTIE: I would like to congratulate Mr. Koontz on what I felt was an excellent presentation and set of results. I think his comments to the end of the last question were along the lines that I tend to think and I wonder if he would comment on the following. I personally and I think many people in my organization dislike, I'm sure others do, the idea of containment standing at high pressure over a prolonged period during which there is the danger that the containment may just fail, just the possibility. Now I think

it was your second slide which showed the decrease in the amount of airborne activity in the vessel. It was quite an impressive decrease, but I think that was for the experimental size vessel. I believe that if you scale up the experimental vessel to full size you get a slower fallout rate. Could you tell me for example how long it takes in a full size containment vessel to get a reduction by a factor of 10 (or some such simple answer please)?

KOONTZ: One of the striking things about our model is that as you increase the height of the vessel for a high concentration, of the order of 100 micrograms/cc, is that the time to decrease the concentration to a given level is not increased as the height increases, but rather it remains more or less constant or even decreases as the height increases. This is attributed to gravitational agglomeration, where if you have a longer time for the particle to fall, its likelihood of collision increases and allows it to grow bigger and thus fall out faster. The one thing that may keep this from continuously increasing forever is the effective density effect, where the agglomeration occurs but particle does not have its ideal density. I have no real rule of thumb about time and reduction factors but I did have one slide to talk about half time which I have over there. Let's say that I do have such information and I can give it to you.

FIRST: I have a question about the last slide you showed indicating concentrations of materials in the atmosphere. This also refers to your last answer. You showed a concentration of 282 micrograms/cc. I wondered if this was a real concentration that was measured or a theoretical one because our experiences in generating aerosols indicates that the maximum concentration that can be attained is considerably lower because of the factors of agglomeration and settling. A second point you might comment on is the assumption of sphericity in your model. As you know and as you have remarked, these particles are far from spheres, either in shape or in density. Are you assuming that the particle size which you are showing on your slides is the size of an equivalent sphere of equal settling velocity or are these measured sizes?

KOONTZ: Let me answer the question about concentration. The values are based on the hypothetical accident in which there is an instantaneous release of the mass into a volume, uniformly distributed and all of those things that can't happen in reality, but we are doing it for the purpose of the parametric study. You are right the particle sizes represent the effective aerodynamic diameter and are so measured, however, we still have to assume a spherical shape in our model, even though we are comparing it to an effective aerodynamic parameter.

PARKER: My question is similar to Dr. First's in that I would ask Mr. Koontz if he shouldn't spend a little discussion on particle behavior where the concentration isn't in this hypothetical maximum. For example, the people that I have talked to usually concede that a factor of 10 less than your maximum value is the top limit that anyone can conceive and actually as far as performing a demonstration I think it's almost a factor of 100 less. In that case wouldn't the settling behavior be more or less linear with the height of the containment?

KOONTZ: That's correct, if you don't have the agglomeration mechanism and you have, let me put it another way, if you don't have high enough particle concentration to cause a considerable amount of agglomeration in a given time, then you have normal settling of an aerosol which is porportional to the velocity and height. This however, is a regime that occurs only if you don't have a high concentration at first. If you start out with a high concentration, it doesn't matter that you are eventually going to get down to a low concentration, the aerosol's memory is based on its initial concentration. If you never have the high concentration in the first place then the danger of the leak is not as great.

ROBERTS: I have a question, but it can wait until the coffee break for your answer. You say that the density of an agglomerate decreases with size, however I have observed large snowflakes falling faster than small ones. How can that be explained?

KOONTZ: Large particles with low density fall faster because the velocity is porportional to both radius and density.

RADIOIODINE FIELD STUDIES WITH SYNTHETIC AEROSOLS[1]

by

D. N. McNelis, S. C. Black and E. L. Whittaker

Radiological Research Program
Southwestern Radiological Health Laboratory

ABSTRACT

The radioiodines are the principal source of human thyroid exposure at early times following the detonation of fission devices. The major pathway for this exposure is the forage-cow-milk chain. With the cessation of atmospheric testing and the reduction in Plowshare activities, simulation remains the primary method to study this pathway. To do this, a series of experiments was conducted in which a radioactive contaminant was released under controlled conditions to simulate the passage of a radioactive cloud over cow forage. Forage is the initial link in the forage-cow-milk-man food chain and in these studies the interrelationship of the physical, chemical and biological variables concerning the transport through that link were investigated. $Na^{131}I$ labeled diatomaceous earth aerosols with count median diameters ranging from 0.2-24.0 μm, a ^{131}I labeled hydrosol and elemental iodine were generated for these studies. The aerosol preparation, labeling, generation and analytical procedures are discussed.

INTRODUCTION

The radioiodines are recognized as the principal source of human exposure at early times following the detonation of a fission device. This is due, primarily, to the relatively high fission yield, rapid transport in the forage-cow-milk pathway, and concentration in the thyroid.

One approach to the study of radioiodine exposures is to set up experiments in the fallout pattern of nuclear tests. If more control of the variables is required, synthetic aerosols may be used. This latter approach has become useful since atmospheric tests have been terminated and since Plowshare cratering tests have been so infrequent.

For controlled studies with radionuclides, a Grade A dairy farm[(1)] was established at the Nevada Test Site (Figure 1). The generation and assessment of a variety of aerosols used to contaminate the cow forage at this farm are the subject of this paper.

PROCEDURES

The procedures used in the studies to be described were designed to meet certain objectives, such as:

(1) Generation of an aerosol with a known particle size distribution,

1. This research performed under Memorandum of Understanding SF-54-373 for the U. S. Atomic Energy Commission

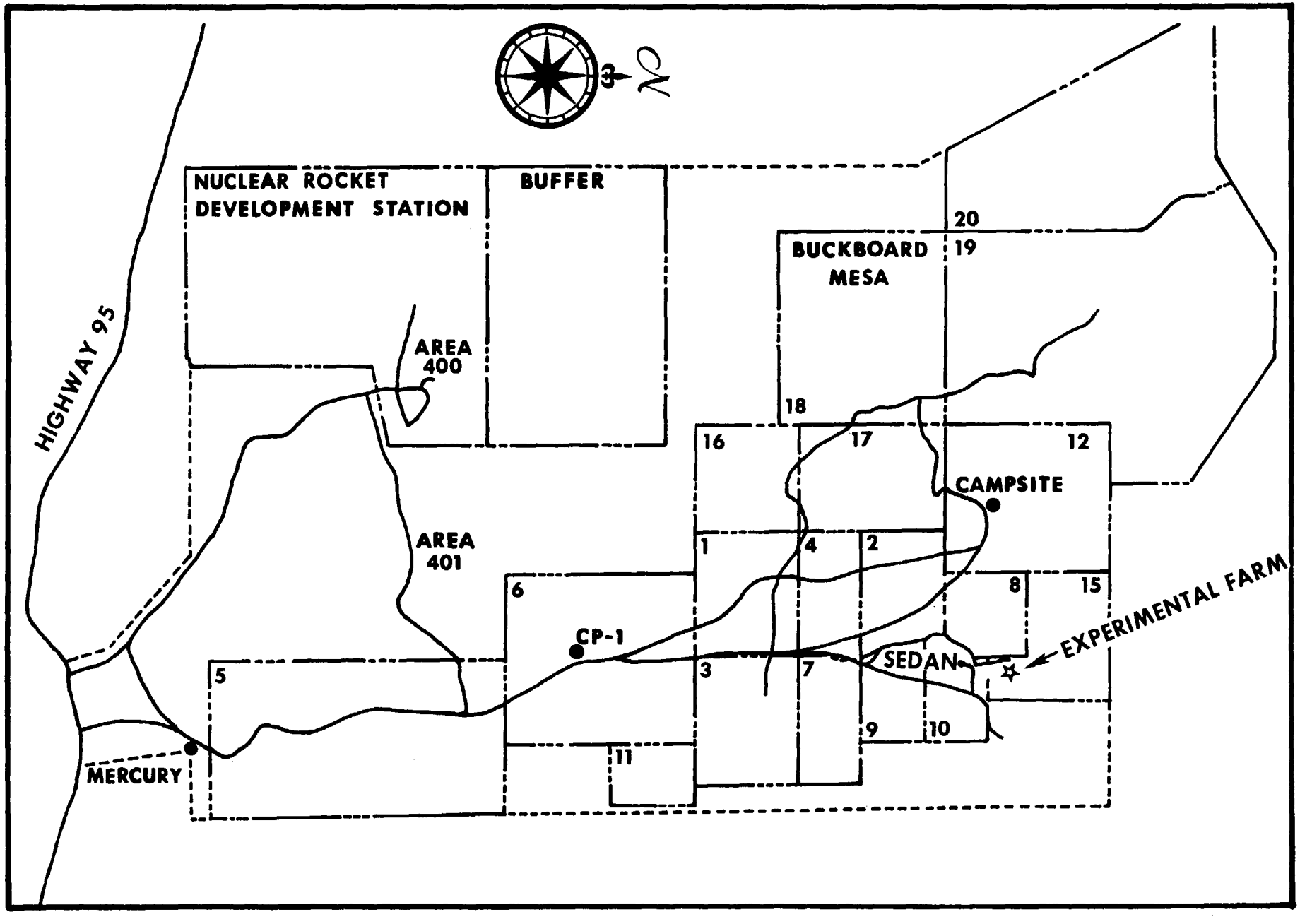

FIGURE 1 — LOCATION OF USPHS FACILITIES ON THE NEVADA TEST SITE

(2) deposition on a certain area sufficient to yield a predetermined $\mu Ci/m^2$ contamination, and

(3) determination of the physical parameters associated with a given deposition of the aerosols.

Five experiments, using aerosols tagged with ^{131}I, have been conducted at the farm as shown in outline in Table 1. The experimental requirements along with some of the actual data in the table indicate the success in meeting those requirements. The desired deposition, in all cases, was 100 nCi/kg or more on the cow forage.

In these experiments, careful consideration was given to the meteorological conditions to minimize their effect on the aerosol generation and deposition. Wind velocity and the relative humidity were prime considerations. Full use was made of the early morning drainage winds characteristic of the area because of their predictability and reproducibility. Wind speeds of less than 4 m/s (9 mph) and a wind direction with an azimuth between 315° and 15° were considered acceptable for these experiments.

The aerosol generator used in these experiments was developed during a series of preliminary tests and has proved satisfactory for our purposes. Figure 2 is a schematic drawing of the generator which was constructed with common laboratory supplies. The glass beads aid in the removal of the aerosol as well as in breaking-up clumps of material. The stainless steel screens at the outlet also helped to reduce clumps of material. Clumping was more of a problem when the relative humidity was high.

The dry aerosols were prepared using a wet-labeling and vacuum-evaporation drying system. A typical preparation procedure was that as used in Project HARE.[2] For this exercise, 10 ml of a source solution, containing 100 mCi of ^{131}I, was added to 7 ml of an aqueous solution containing 0.7 mg of NaI. Then 0.5 ml aliquots were transferred to each of 32 two-ounce bottles containing 1 ml of 1M $Na_2S_2O_3$, 5 ml of 2M Na_2CO_3 and 25 ml of water. The contents of these bottles were added to approximately 30 ml of water, 450 ml of isopropanol, 7 g of glass beads and 150 g of the prepared diatomaceous earth (DE). After mixing, the material was dried using a vacuum-evaporation system. The evaporation rate of the flasks' contents was controlled to prevent the boiling action from becoming too violent. The total drying time for this study was 40 hours with the flasks being heated by hot tap water for the last 18 hours to insure efficient drying. Depending on the particle size desired, mechanical screening or ball-milling or a combination are used to pretreat the particulates.

The preparation for the MICE experiment, the gaseous $^{131}I_2$ release, was similar to that employed by the National Reactor Testing Station (NRTS).[3] Four vials containing various solutions were added in sequence to the generating flasks. The first contained 1.5 mg of NaI carrier, 0.5 ml of H_3PO_2, and 10 ml of distilled water along with the ^{131}I activity. The second contained 130 ml of 2N H_2SO_4. The third was used to initiate the reaction and consisted of 30 mg of $NaNO_2$ and 10 ml of distilled water. The fourth contained the post-generation reducer solution (to stop the I_2 generation)

Table 1. Outline of Five Experiments Using ^{131}I Aerosols

Project Name	Carrier Aerosol	Desired Size (μm)	Measured (CMD-μm)	Forage Type	Deposition μCi/m^2
Hayseed	Diatomaceous earth	20	23	Sudan grass	3.1
Alfalfa	Diatomaceous earth	1-5	2.0	Alfalfa	4.7
HARE	Diatomaceous earth	<1	.60	Alfalfa and Sudan grass	1.3
SIP	Diatomaceous earth	<1	.13	Alfalfa	1.6
MICE	Air	gas		Alfalfa	.66

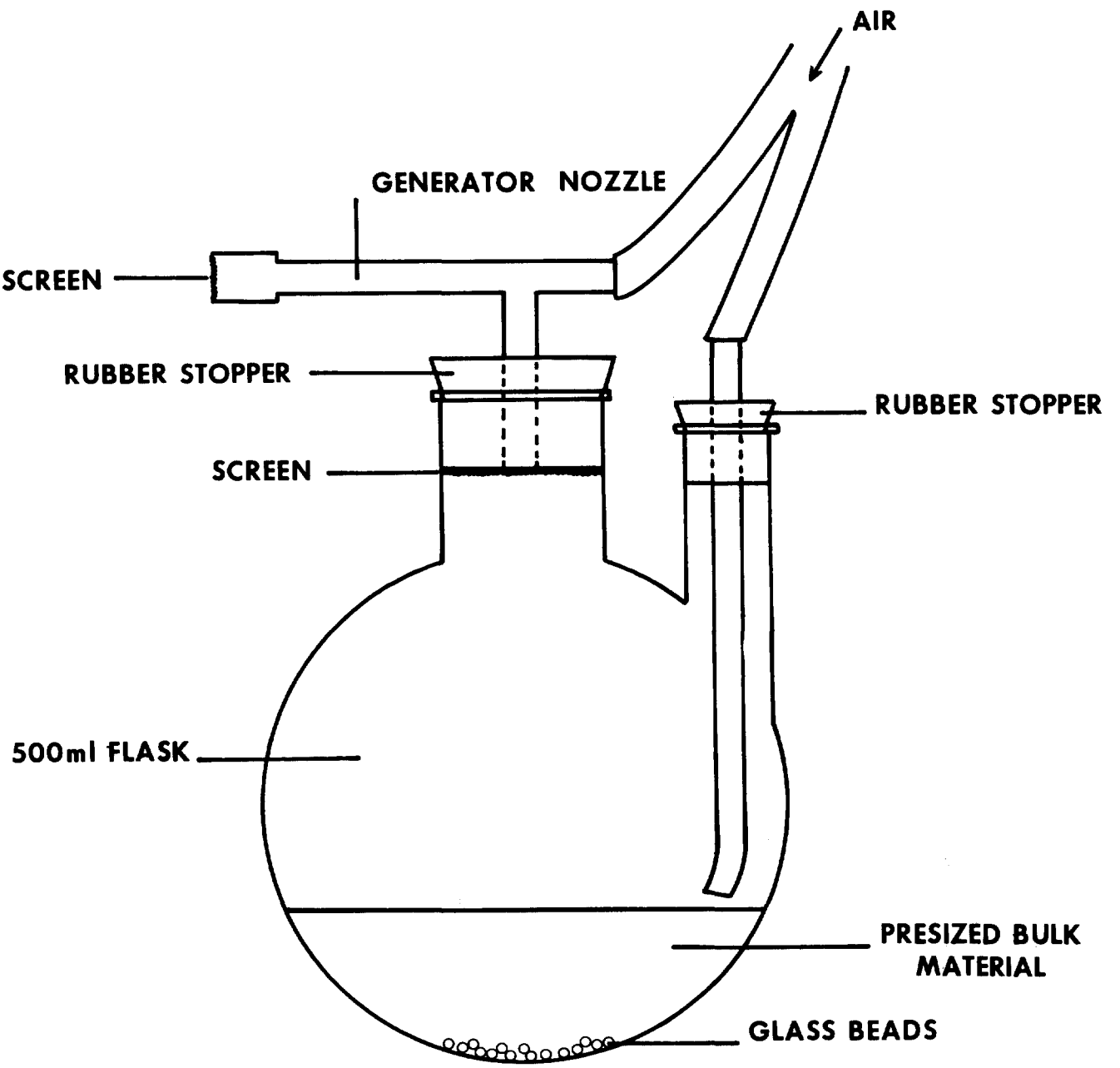

FIGURE 2 — AEROSOL GENERATOR

which consisted of 5 ml of 30% H_3PO_2 and 5 ml of distilled water. The generating flasks for this release were modified to include a fritted glass sparging tube at the inlet and had the exhaust tube loosely packed with glass wool. To generate I_2, the acidic solution of $Na^{131}I$ was oxidized and the $^{131}I_2$ was sparged from the solution with nitrogen gas. Generation of the gaseous materials was regulated to last for approximately 30 minutes.

To obtain the many deposition parameters required to adequately describe the aerosol releases, many types of samples were collected. These included:

(1) Planchets - stainless steel 0.01 m^2 planchets coated with a non-setting resin. These are used to determine the $\mu Ci/m^2$ deposited and for deposition velocity calculations.

(2) Glass slides - specially cleaned glass microscope slides used for particle size distribution studies.

(3) Air samplers - 10 cfm air samplers equipped with prefilters and charcoal cartridges for determining air concentration and particulate to gaseous ratios.

(4) Special air samplers - modified sampling train, e.g., charcoal impregnated paper, used for special aerosol measurement.

(5) Cascade impactors - Unico* type used for certain particle size measurements.

(6) Planchet racks - racks holding planchets at various heights and angles and used to determine the radioactive profile of the aerosol cloud.

A typical sampling grid is shown in Figure 3 which is the actual experimental arrangement for Project HARE.[2]

The particle size distribution was determined from the Feret diameter measurement,[4] using optical and electron microscopes, and was characterized by the count median diameter (CMD). The filter/charcoal ratio used in Table 2 is just the ratio of the total activity collected on each. The data from the air samplers were used to calculate the integrated air concentration (units of $\mu Ci\text{-}s/m^3$) by dividing the sum of the prefilter and charcoal activities by the air flow rate. The planchet deposition ($\mu Ci/m^2$) divided by the integrated air concentration gives the deposition velocity (m/s).

RESULTS AND DISCUSSION

Selected results from the five experiments under consideration are shown in Table 2 and are briefly discussed in the following paragraphs.

The equal deposition lines (isopleths) for Project Hayseed[5] are shown in Figure 4, and are based on the planchet data. The CMD as determined from the optical sizing of the particles on the glass slides was 23 μm. The small areas shown at the leading edge of the test grid were for piled green

* Unico Cascade Impactor for Simplified Particle Size Analysis, Manufactured by Union Industrial Equipment Corporation, Port Chester, New York.

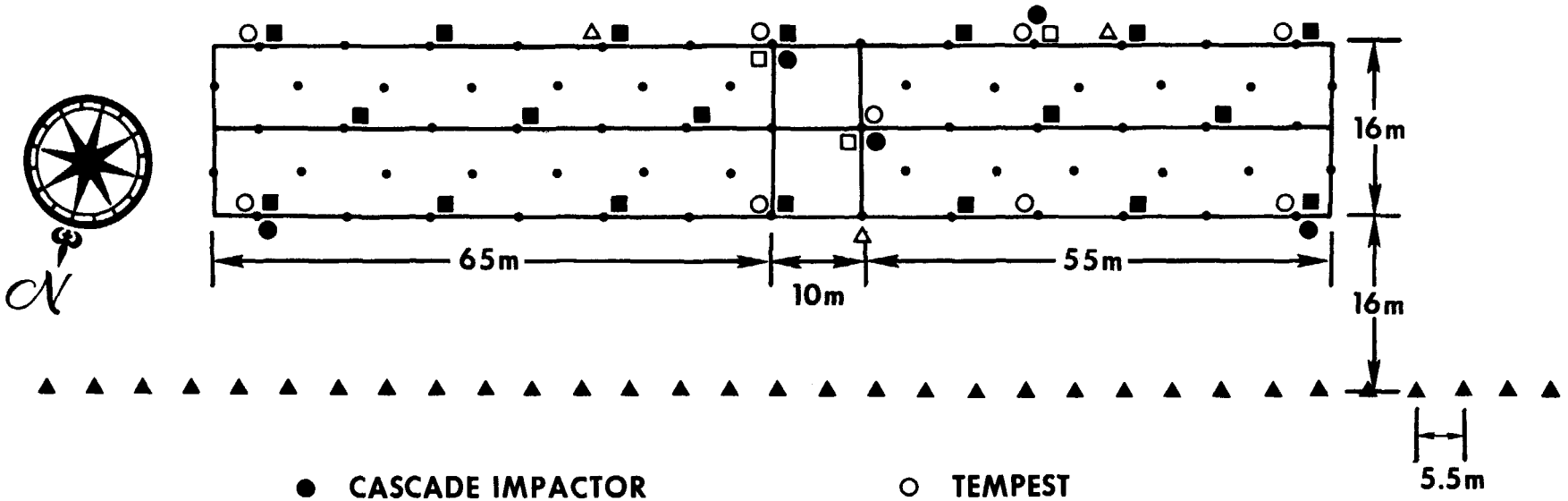

● CASCADE IMPACTOR
□ FILTER PACK
△ PLANCHET RACK
■ GLASS SLIDE
○ TEMPEST
• PLANCHET
▲ GENERATOR

FIGURE 3 — TYPICAL SAMPLE GRID

Table 2. Summary of Results from Five Controlled Experiments

Measured or Calculated Parameter	Experiment Title					
	Hayseed	Alfalfa	HARE		SIP	MICE
Particle size-μm	23	2.0	.60		.13	Gas
Forage type	Sudan	Alfalfa	Sudan	Alfalfa	Alfalfa	Alfalfa
Average deposit-μCi/m^2	3.1	4.7	1.2	1.4	1.6	.66
Percent deposit	21	13	5.0		4.0	1.8
Air concentration-μCi-s/m^3	322	33.4	88.0		157	129
Filter/Charcoal ratio	4.9	3.5	1.0		3.2	.12
Deposition velocity-cm/s	.96	1.4	1.4	1.6	1.0	.51
Peak in milk-nCi/liter	75.9	237	21.6	50.8	68.4	151
Milk/Forage ratio	.028	.070	.021	.066	.061	.058

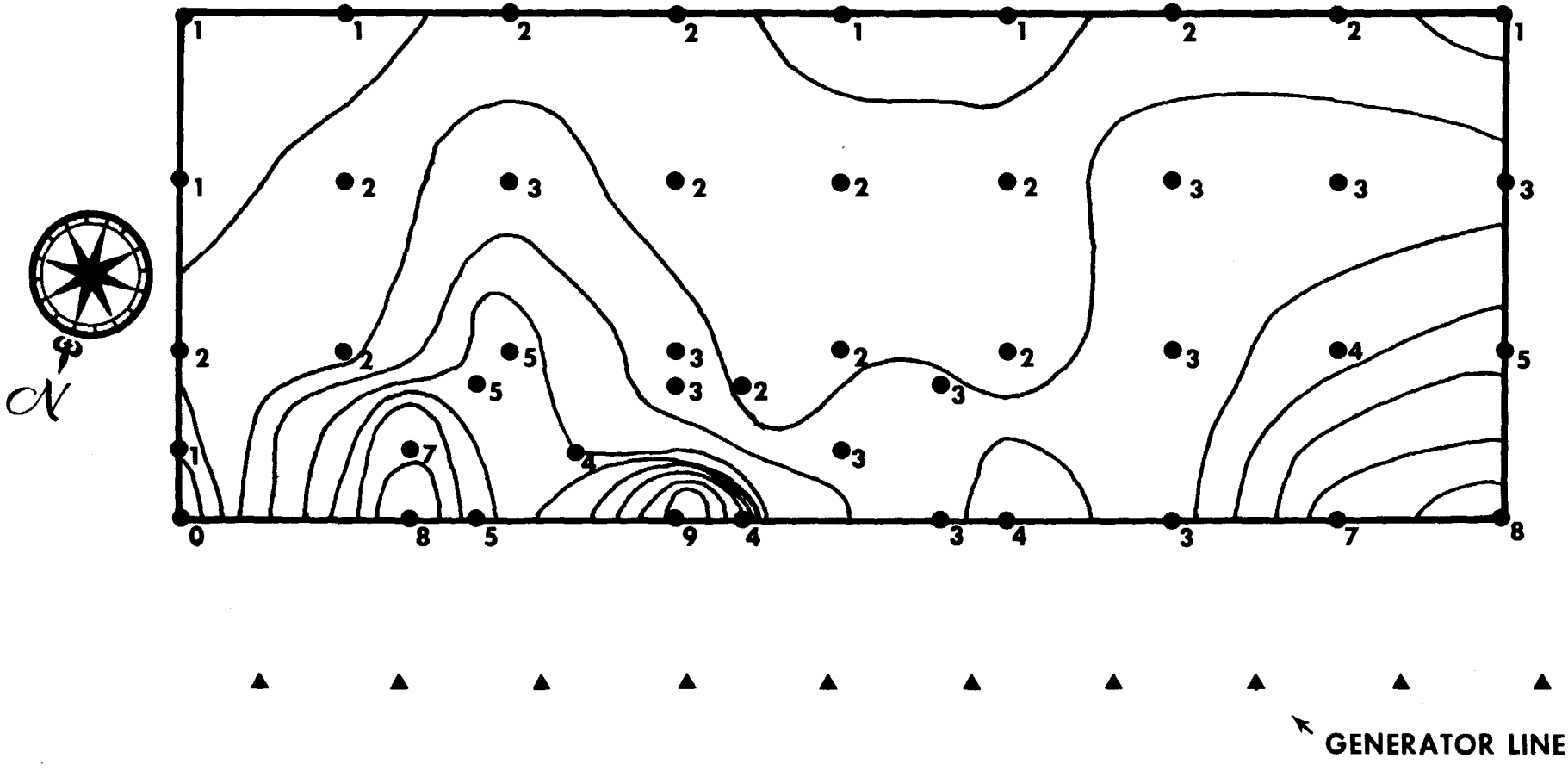

FIGURE 4 — PROJECT HAYSEED ^{131}I ACTIVITY ($\mu Ci/m^2$) ISOPLETHS FROM PLANCHET DATA

chop, piled hay, and cows in stanchions and were used for special studies. The major crop for this study was Sudan grass and the average deposition for the entire grid was 3.1 $\mu Ci/m^2$. Approximately 21% of the total radioiodine labeled aerosol released was deposited on the 600 m^2 test grid. The lateral distribution as can be seen from this figure appears quite uniform and the drop in activity from the front of the plot to the rear is consistent with the large CMD of the particulates.

The contribution to the radioactivity in the milk resulting from air uptake amounted to only about 1% for this study. This is in good agreement with the results found in Project Alfalfa where the air uptake contribution was calculated to be about 2%.[6] Subsequent tests (Projects SIP and MICE) confirm the contribution via this pathway to be minimal.

The deposition results for Project Alfalfa are shown in Figure 5. The CMD of this aerosol was calculated as 2.0 μm from the size distribution data which are shown in Figure 6. The planchet data yielded an average deposition value of 4.7 $\mu Ci/m^2$ and approximately 13% of the activity generated was deposited on the test grid. As would be surmised, the distribution for the smaller sized aerosol is more uniform over the study plot, as compared to Hayseed.

Project HARE, the third study in the series of decreasing particle sizes, had as an additional objective, determining whether aerosol particle size or forage species was the main contributor to the difference in the milk to forage ratios from the first two experiments. This ratio for Project Alfalfa was approximately four times the ratio for Project Hayseed.

The deposition isopleths are shown in Figure 7, for the two test grids used in HARE, one crop being Sudan grass and the other alfalfa. The activity deposited on the field averaged 1.25 $\mu Ci/m^2$ for the Sudan grass plot and 1.43 $\mu Ci/m^2$ for the alfalfa study plot. Approximately 5% of the activity in the generator flasks was deposited on the test grid as estimated from the planchet data. This lower percentage deposited conforms to the decrease in particle size. The CMD of this aerosol was 0.6 μm.

The milk-to-forage ratio and percent in milk were both lower for Sudan-fed cows than for alfalfa-fed cows and the relative magnitudes agreed with similar data in the other experiments. These results suggest that forage type rather than particle size is responsible for the lower milk-to-forage ratio and lower percent in milk in Sudan-fed cows.

The smallest CMD aerosol studied in this series was 0.13 μm used during Project SIP.[7] Electron microscopy was used in addition to the optical microscopy to size this fine aerosol. The planchet values showed that the average deposition over the study area was 1.6 $\mu Ci/m^2$ and was by far the most uniform of any of the releases. The isopleths drawn from the planchet data (Figure 8) indicate that 96% of the test grid was contaminated at levels of from 1-3 $\mu Ci/m^2$ and the remaining 4% at a level of 4.5 $\mu Ci/m^2$. Approximately 4% of the total activity was deposited on the study area. The data from the planchet racks together with the respective "deposition vectors" are shown graphically in Figure 9. The deposition vector is defined as the resultant of the two vectors calculated from the activity on the horizontal and vertical planchets. These data demonstrate that the active

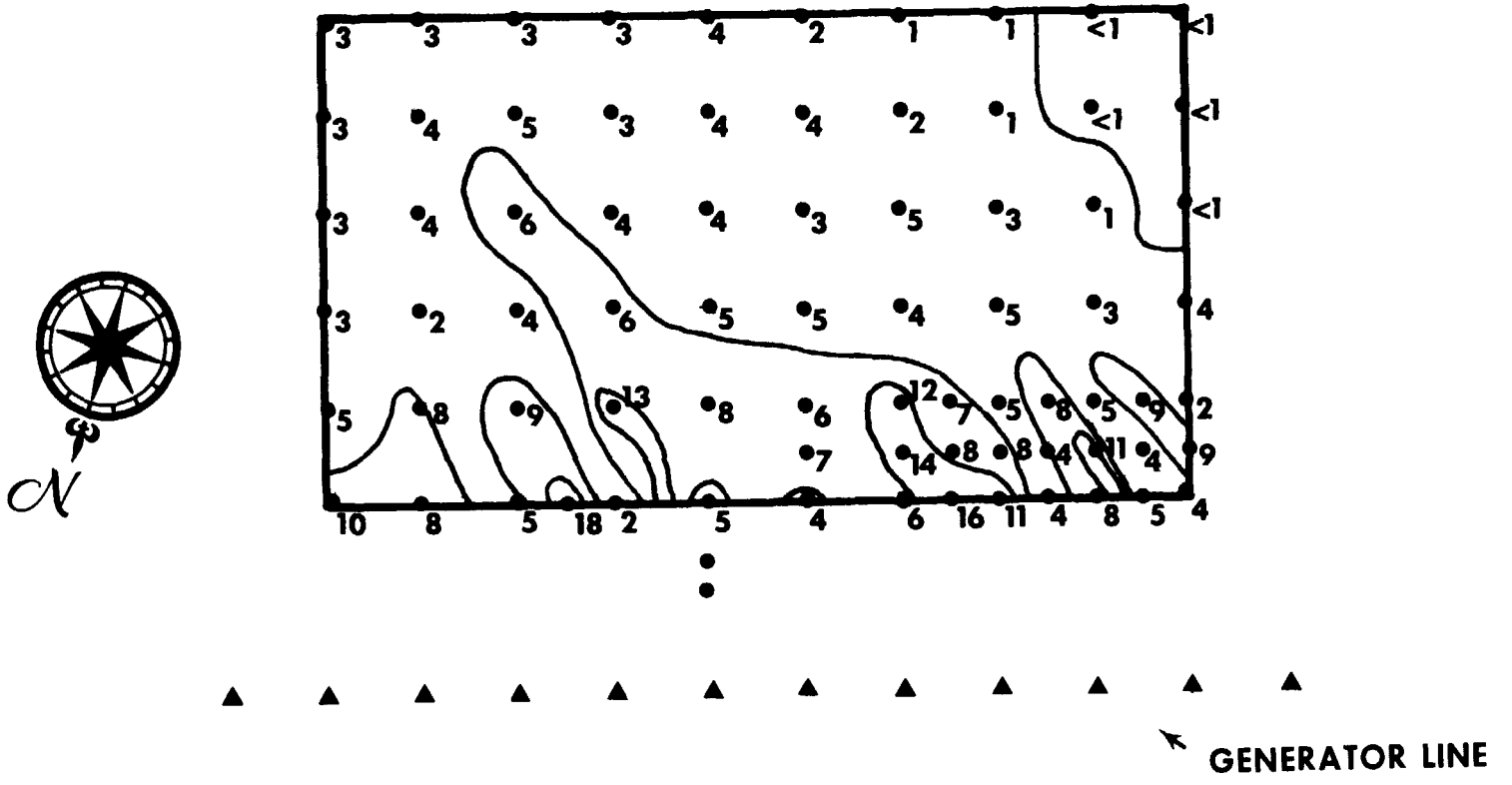

FIGURE 5 — PROJECT ALFALFA ^{131}I ACTIVITY ($\mu Ci/m^2$) ISOPLETHS FROM PLANCHET DATA

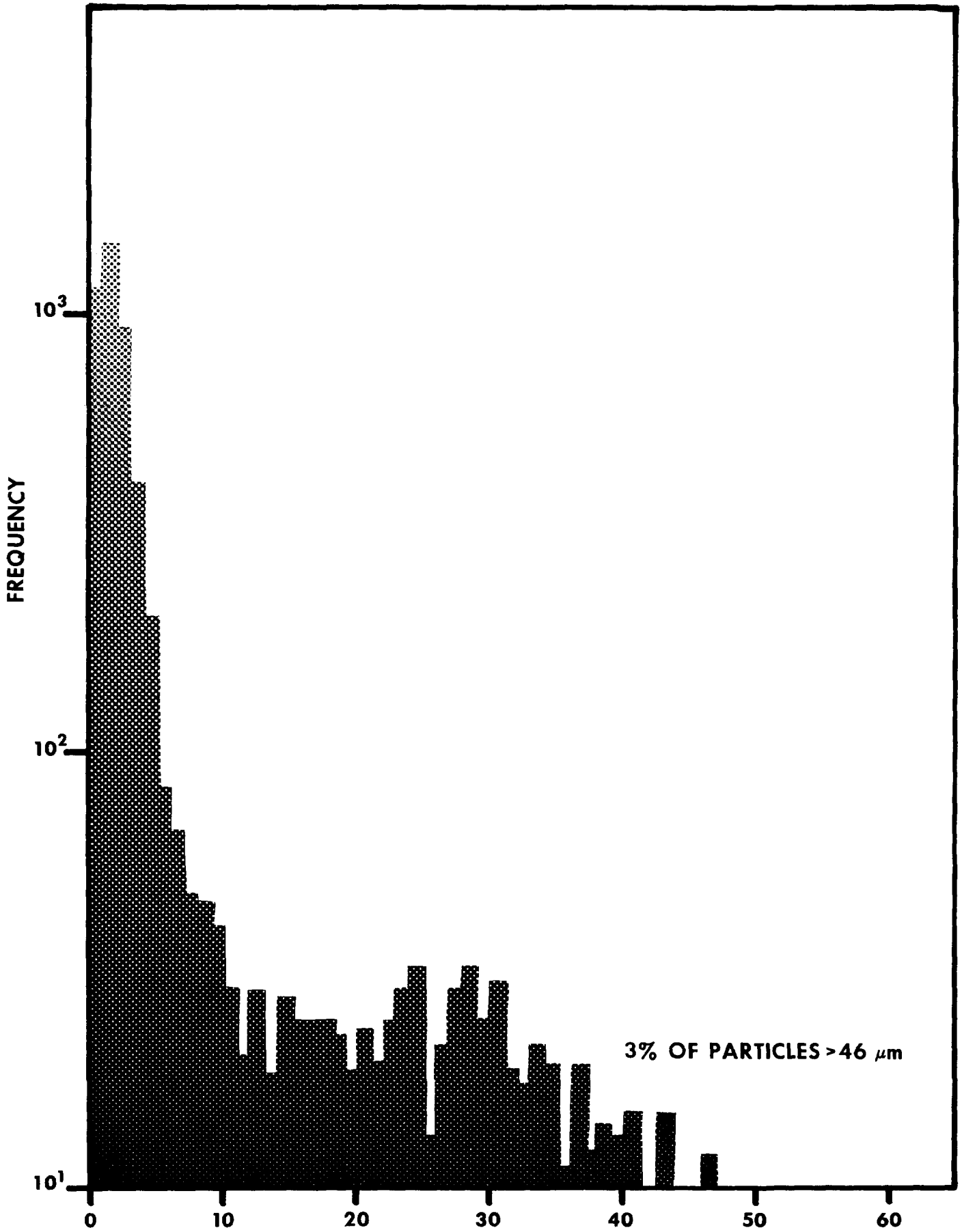

FIGURE 6 — PARTICLE SIZE DISTRIBUTION HISTOGRAM

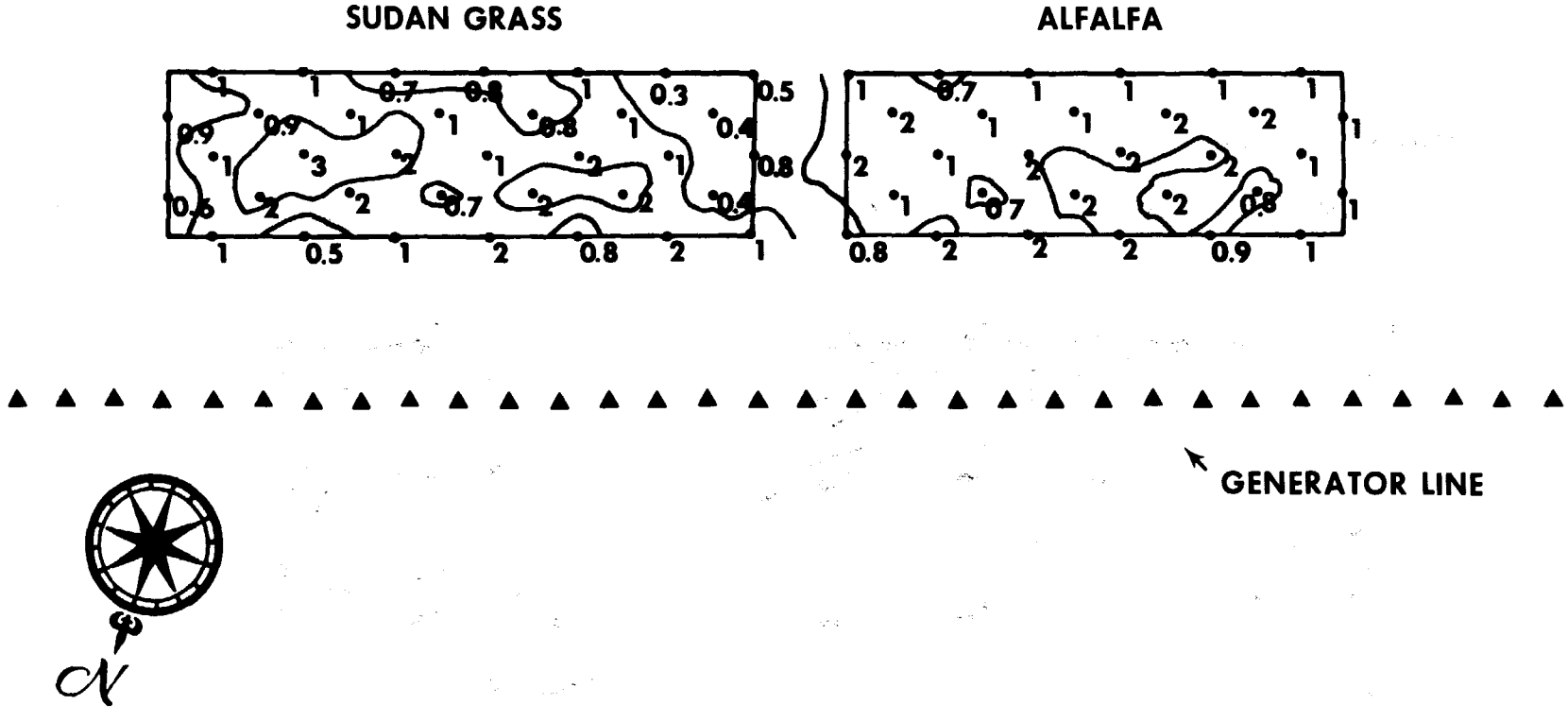

FIGURE 7 — PROJECT HARE ^{131}I ACTIVITY ($\mu Ci/m^2$) ISOPLETHS FROM PLANCHET DATA

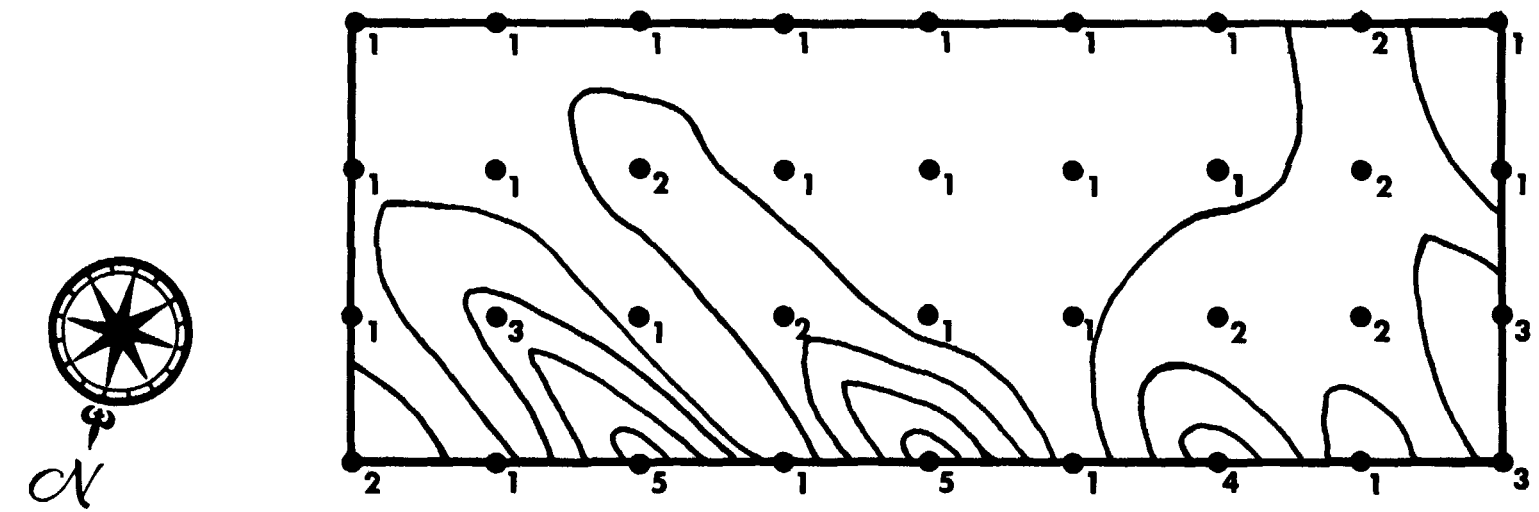

FIGURE 8 — PROJECT SIP ^{131}I ACTIVITY ($\mu Ci/m^2$) ISOPLETHS FROM PLANCHET DATA

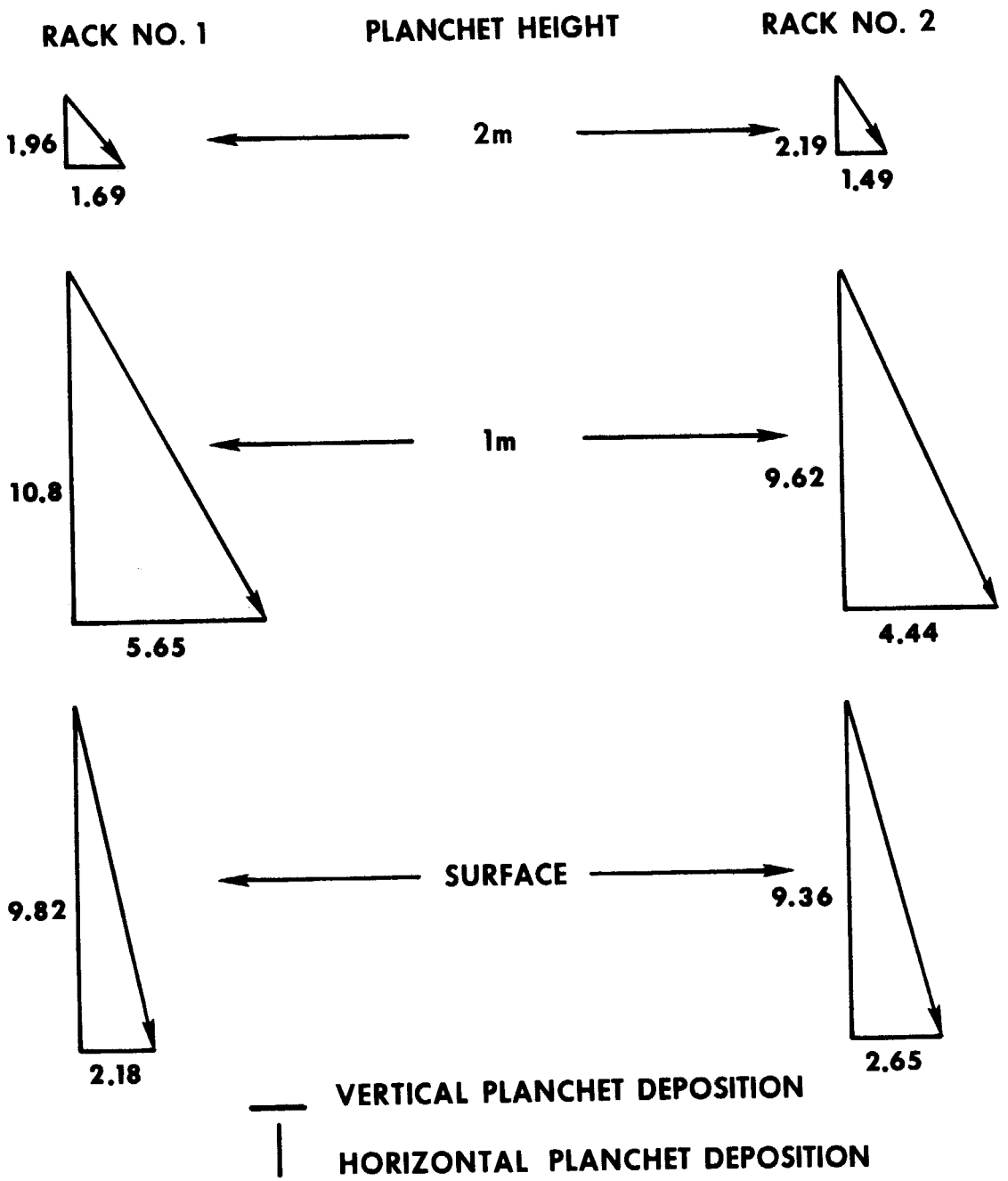

FIGURE 9 — PROJECT SIP PLANCHET RACK DATA ($\mu Ci/m^2$) AND DEPOSITION VECTORS

cloud remained close to the ground, i.e., in the first meter during transport across the experimental area. The activity on the two meter elevation planchets dropped off markedly. The vector shows that the particles were being deposited in a nearly vertical mode close to the ground whereas at higher elevations the horizontal vector became stronger, probably due to the effect of the winds. The uniformity of the individual values between the two planchet racks separated by some 30 meters is remarkable.

The activity isopleths from Project MICE,[8] are shown in Figure 10 and indicate an average deposit of 0.66 $\mu Ci/m^2$. The three special air samplers were used on this study to confirm that $^{131}I_2$ was being generated.

The AC-1 charcoal impregnated filter paper has a high collection efficiency for elemental iodine but, at the flow rates used, would be inefficient for collecting CH_3I and HI because of the short residence times. An average of 86% of the activity collected by these samplers was found on the AC-1. An additional 12% was found on the Microsorban prefilter indicating the presence of some particulates. Microscopic examination of glass slides and electron microscope grids yielded a CMD of 0.01 μm for the particulates collected. The Unico Cascade Impactors, used on this study, yielded a mass median diameter (MMD) (1.6 μm) of the sampled aerosol. A CMD can be calculated from this value and also indicated a value of 0.01 μm.

The peak ^{131}I milk concentrations, from cows on fresh forage, obtained in these experiments are plotted on Figure 11 against the integrated air concentration divided by filter-to-charcoal ratios. In addition to the values for these studies, the results of two nuclear explosions are included, i.e., Pin Stripe and Palanquin. Although the levels are higher in the milk for the controlled releases, the data demonstrate that the controlled field releases yield data that correlate with actual fallout data. The values, one from cows fed green chopped alfalfa and one from cows fed baled hay, from Project MICE appear somewhat out of line, but that release, being primarily gaseous, was not representative of a true aerosol. The straight line plotted in the figure is best fit to the data and the deviation plotted is within a factor of ±2. It can also be inferred from these data that the iodine is as available from the controlled releases as it is from the event-related aerosols.

Figure 12 is a plot of the particle size of the aerosol versus the deposition velocity. This latter value is calculated from the deposition on the planchets divided by the integrated air concentration at the same location. Two points are plotted for the Project HARE experiment, one for each type of forage used. The lower deposition velocity for the 23 μm aerosol (Hayseed) suggests that air bouyancy exerts some effect on large particles of these aerosols. The data for Project MICE, deposition velocity of 0.51, is in close agreement with the average value of 0.65 reported for the first two Controlled Environmental Radioiodine Tests conducted at the National Reactor Testing Station.[9] The elemental iodine was generated in the same manner during those studies.

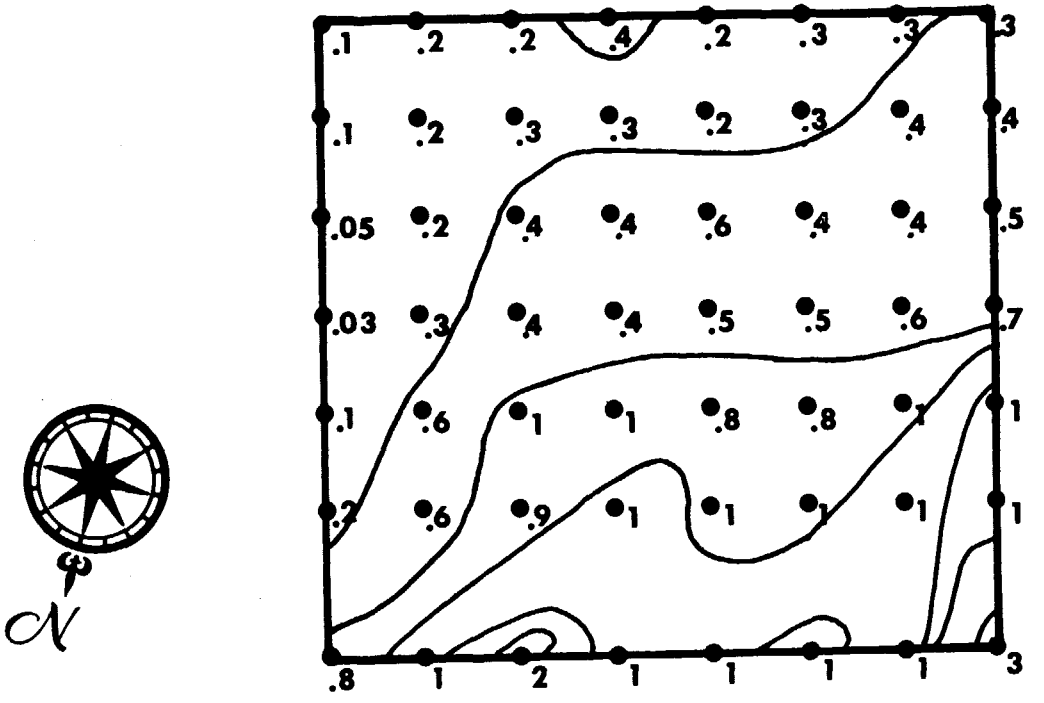

GENERATOR LINE

FIGURE 10 — PROJECT MICE I ACTIVITY (μCi/m^2) ISOPLETHS FROM PLANCHET DATA

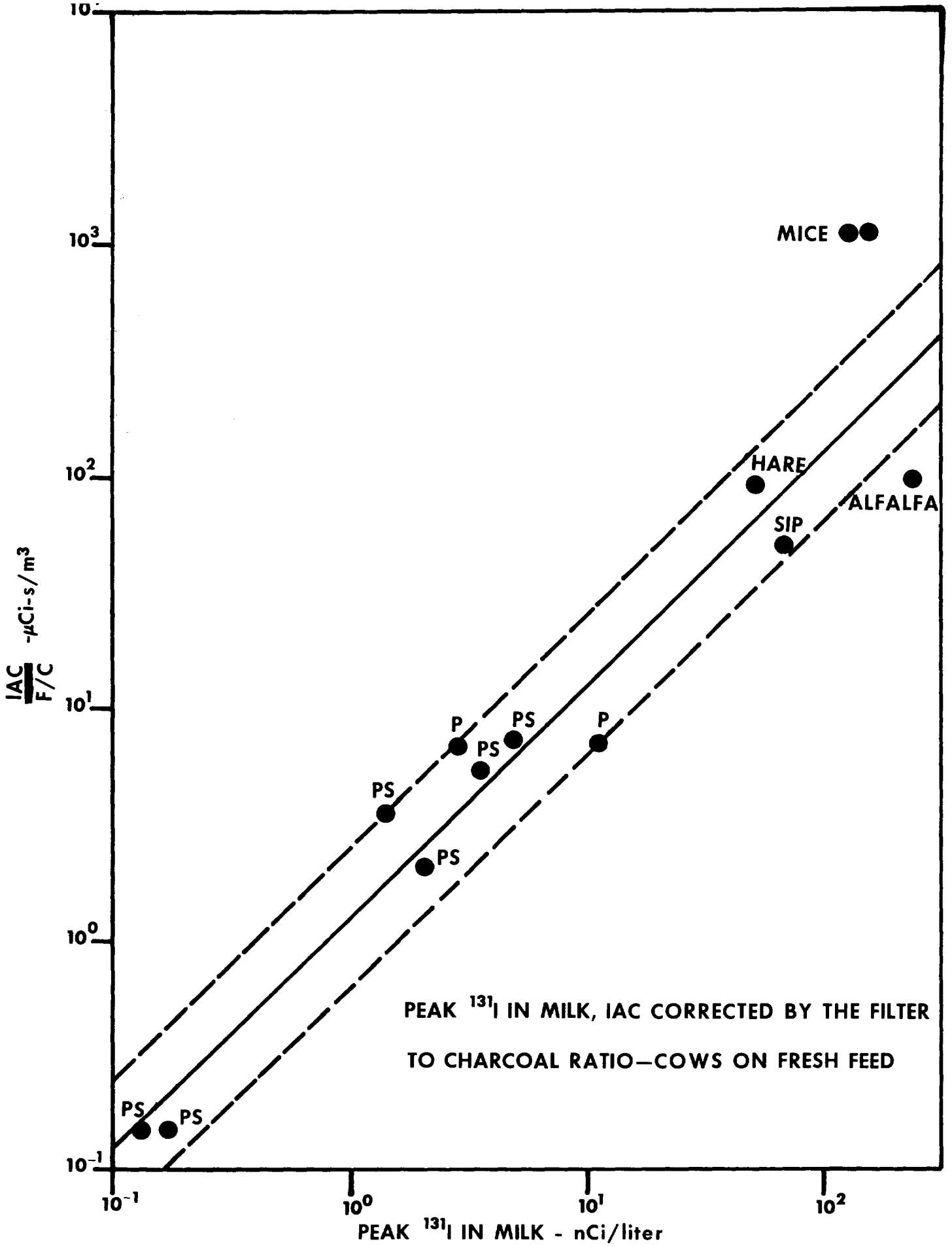
MICE
HARE
ALFALFA
SIP
P
PS
PS
PS
PS
P
PS
PS
PEAK ^{131}I IN MILK, IAC CORRECTED BY THE FILTER
TO CHARCOAL RATIO—COWS ON FRESH FEED
$\frac{IAC}{F/C}$ -μCi-s/m^3
10^3
10^2
10^1
10^0
10^{-1}
10^{-1}
10^0
10^1
10^2
PEAK ^{131}I IN MILK - nCi/liter

FIGURE 11

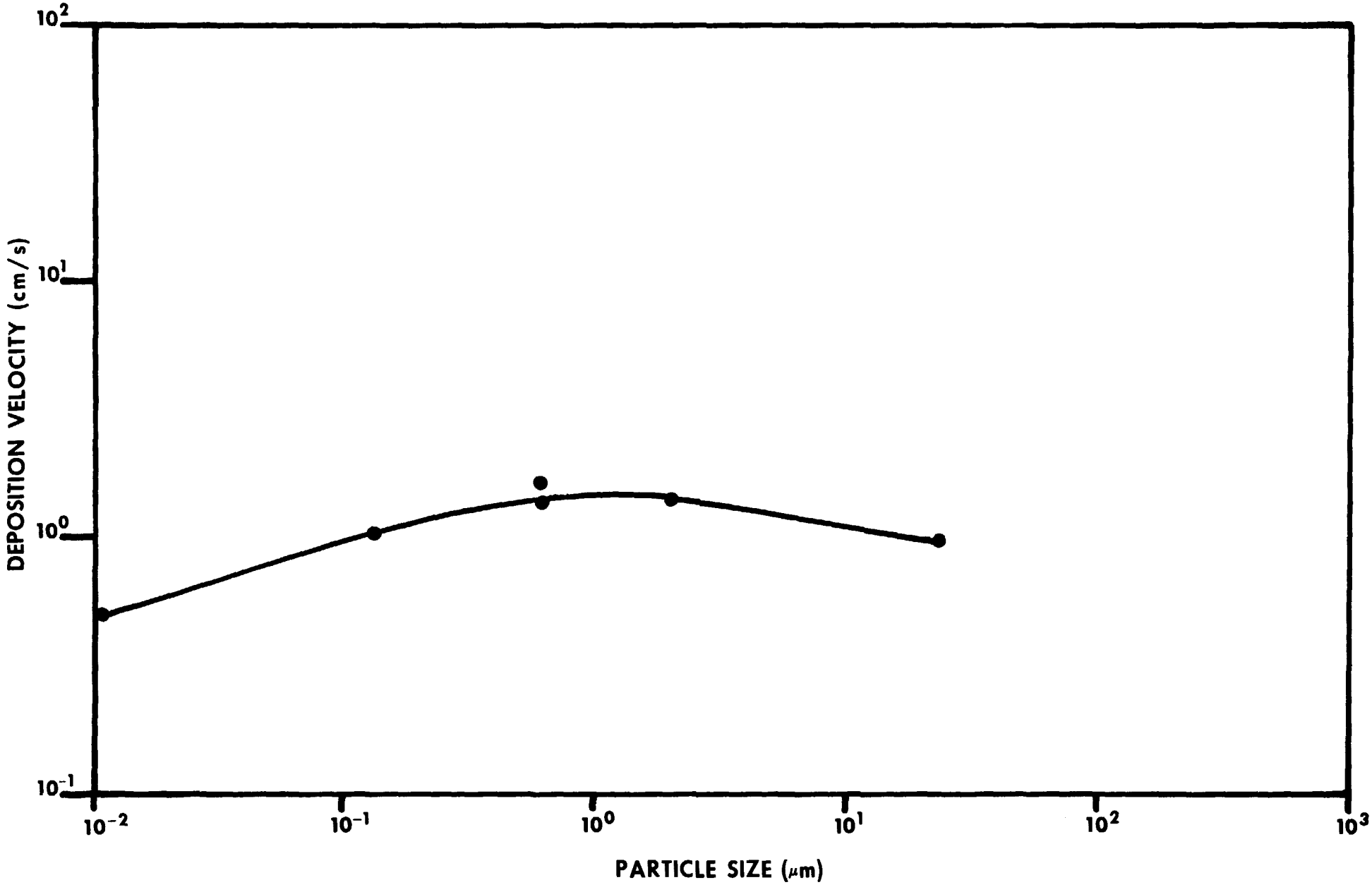

FIGURE 12 — PARTICLE SIZE VERSUS DEPOSITION VELOCITY FOR FIVE ^{131}I CONTROLLED RELEASES

Finally, on two studies, Projects Hayseed and HARE, the ratio of the deposition actually found on two types of forage to the value estimated from the planchet data was calculated. On Sudan grass, this ratio was 3.28 for Project Hayseed and 1.46 for Project HARE. On alfalfa, these values were 2.81 and 1.66 for the two studies, respectively. Since forage is a three dimensional sampler, the ratio would be expected to be greater than unity.

CONCLUSIONS

1. Aerosols of known particle size distribution can be generated in such a manner as to yield a known activity deposition level.

2. Lateral deposition was uniform for these studies and the downwind distribution was a function of the particulate size as expected.

3. The deposition velocity value can be used to estimate the aerosol particle size over a range of diameters.

4. Planchets can be used to estimate the activity per kilogram to be expected in forage. This estimation is more sensitive to particle size than it is to forage type.

REFERENCES

1. R. L. Douglas, Status of the Nevada Test Site Experimental Farm, Southwestern Radiological Health Laboratory, Las Vegas, Nevada, SWRHL Report, SWRHL-36r, 1967.

2. R. H. James, D. N. McNelis, E. L. Whittaker and N. C. Kennedy, Aerosol Preparation, Generation and Assessment (Project HARE), SWRHL Report, SWRHL-75r, Las Vegas, Nevada, 1970.

3. C. A. Hawley, Jr., C. W. Sill, G. L. Voelz and N. F. Islitzer, Controlled Environmental Radioiodine Tests at the National Reactor Testing Station, IDO-12035, Idaho Operations Office, June 1964.

4. L. R. Feret, Association International pour l'essai des Mat. 2, Group D, Zürich, 1931.

5. Bioenvironmental Research, ^{131}I Dairy Cow Uptake Studies Using a Synthetic Dry Aerosol (Project Hayseed), SWRHL Report, SWRHL-28r, Las Vegas, Nevada, to be published.

6. R. E. Stanley, S. C. Black and D. S. Barth, ^{131}I Dairy Cow Studies Using a Dry Aerosol (Project Alfalfa), SWRHL Report, SWRHL-42r, Las Vegas, Nevada, 1969.

7. Bioenvironmental Research, ^{131}I Dairy Cow Uptake Studies Using a Submicron Synthetic Dry Aerosol (Project SIP), SWRHL Report, SWRHL-39r, to be published.

8. R. L. Douglas, Radioiodine Transport Through the Air-Forage-Cow-Milk System Using a Gaseous $^{131}I_2$ Contaminant, paper presented at the 14th Annual Meeting of the Health Physics Society, Pittsburgh, Pennsylvania, June 8-12, 1969.

9. D. R. Adams, D. F. Bunch, W. P. Gammill, C. A. Hawley, Jr., E. H. Markee and M. W. Tiernan, Controlled Environmental Radioiodine Tests at the National Reactor Testing Station, 1965 Progress Report, IDO-12047, Idaho Operations Office, February 1966.

DISCUSSION

JUNKINS: Early in your speech sir I believe you mentioned you were seeking 100 nanocuries per kilogram, was that per kilogram of milk?

McNELIS: No sir, that is on the forage.

JUNKINS: I wonder also how do your results compare with the findings of the British Research Medical Council and perhaps with assumptions of the Federal Radiation Council?

McNELIS: I believe quite closely. These data are being prepared into a prediction model which is now in draft form and will include both the controlled release studies and the Plowshare event studies. Dr. Black of our laboratory is preparing it and it should be out in the near future although one more controlled release may be necessary.

JUNKINS: One last question if I may, the very last slide, figure 12 I think it was numbered, taxed my eye power; I couldn't read the units on the ordinates.

McNELIS: One was deposition velocity and the other particle size. I will give you a copy of this afterward.

CRAIG: I wonder if you have made a comparison between the particle size distribution actually generated by your aerosol generator and that as detected by the methods that you use for your sample evaluations?

McNELIS: Yes sir, we've done a number of these studies. For all of the dry aerosols the size distribution found at any location is reported from an actual sizing of the particulate material found on the glass slides placed at those locations. As far as the total aerosol is concerned we do loose a large fraction of our aerosol either in front of or behind the test grid. This is especially true when we generate the large particles where many of them fall out between the generation line and the front of the test grid. We have also conducted studies where we have tested certain filters of reported efficiency for certain sized particles against known size aerosol distributions.

CRAIG: The real reason I asked this question is that you talked about generating an aerosol from pre-sized material which you had put into a flask, presumably in a suspension of some sort, and then nebulized.

If so, the resulting aerosol is extremely unlikely to have a particle size distribution that bears any relation to the particle size distribution of the "pre-sized" material.

McNELIS: It was aerosolized dry.

CRAIG: In this case, there is even less chance of getting the particle size distribution you started off with, due to the difficulty of breaking up aggregates.

KOONTZ: In your plot of depositions of velocity versus size, I wasn't sure that the size was that of the generated aerosol or the size at the deposition site.

McNELIS: At the deposition or sampling site.

BEATTIE: I just wanted to comment very briefly on the first question. The first questioner mentioned the assumptions made by the British Medical Research Council. Strictly speaking, these are not assumptions; they were results of measurements after the Windscale accident, measurements by Arthur Chamberlain at Harwell and so on and so forth, but not assumptions.